Research and Development Technical Report
SLCET-TR-0941-F

HIGH POWER/HIGH TEMPERATURE BATTERY DEVELOPMENT

S.J. Specht
N. Shuster

Westinghouse Electric Corporation
Naval Systems Division
18901 Euclid Ave.
Cleveland, Ohio 44117

September 1992
Final Report for Period September 1989 - July 1992

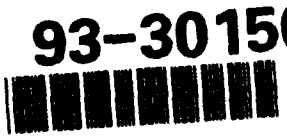

Prepared for
Electronics Technology and Devices Laboratory

US ARMY
LABORATORY COMMAND
FORT MONMOUTH, NEW JERSEY 07703-5601

NOTICES

Disclaimers

The findings in this report are not to be construed as an official Department of the Army position, unless so designated by other authorized documents.

The citation of trade names and names of manufacturers in this report is not to be construed as official Government endorsement or approval of commercial products or services referenced herein.

REPORT DOCUMENTATION PAGE

Form Approved
OMB No. 0704-0188

1. AGENCY USE ONLY (Leave blank)	2. REPORT DATE	3. REPORT TYPE AND DATES COVERED
	September 1992	Final Report: Sep 89 to Jul 92

4. TITLE AND SUBTITLE
HIGH POWER/HIGH TEMPERATURE BATTERY DEVELOPMENT

5. FUNDING NUMBERS
C: DAAL01-89-C-0941
PE: 62705
PR: 1L162705AH94
TA: 11
WU: 01

6. AUTHOR(S)
S.J. Specht and N. Schuster

7. PERFORMING ORGANIZATION NAME(S) AND ADDRESS(ES)
Westinghouse Electric Corp.
Naval Systems Division
18901 Euclid Ave.
Cleveland, Ohio 44117

8. PERFORMING ORGANIZATION REPORT NUMBER
CLIN 0003AB

9. SPONSORING/MONITORING AGENCY NAME(S) AND ADDRESS(ES)
US Army Laboratory Command (LABCOM)
Electronics Technology and Devices Laboratory
ATTN: SLCET-PR
Fort Monmouth, NJ 07703-5601

10. SPONSORING/MONITORING AGENCY REPORT NUMBER
SLCET-TR-89-0941-F

11. SUPPLEMENTARY NOTES

12a. DISTRIBUTION/AVAILABILITY STATEMENT
Approved for public release; distribution is unlimited.

12b. DISTRIBUTION CODE

13. ABSTRACT (Maximum 200 words)

The lithium (alloy)/cobalt disulfide (Li-alloy/CoS_2) electrochemistry is currently under development at Westinghouse as a high-power, pulsed energy source for mobile electric weaponry. The goals of this LABCOM sponsored program were to optimize both cell components and operating conditions. Candidate cathode materials were investigated, and only CoS_2 was identified as having excellent characteristics when operated in its higher voltage region. Alternate disulfides and chalcogenides could not match CoS_2 for pulse performance and open circuit stand capability. Separator materials were investigated as replacements for the baseline Maglite D MgO. Silicon nitride, yttria, Magox Super Premium MgO and sintered, porous AlN were identified as suitable candidiates for qualification as Maglite D replacements. The AlN was a dimensionally stable material and exhibited very low residual or final currents. Cells were redesigned and tested based upon the above findings. The cycle life goal of 200 cycles was achieved with cells employing the reduced quantities of the active materials. The best cell tested exceeded 350 cycles and 2500 individual 4-second pulses.

14. SUBJECT TERMS	15. NUMBER OF PAGES
Molten salt battery systems; pulse power; lithium; metal sulfide	51
	16. PRICE CODE

17. SECURITY CLASSIFICATION OF REPORT	18. SECURITY CLASSIFICATION OF THIS PAGE	19. SECURITY CLASSIFICATION OF ABSTRACT	20. LIMITATION OF ABSTRACT
Unclassified	Unclassified	Unclassified	UL

TABLE OF CONTENTS

LIST OF FIGURES

LIST OF TABLES

High Temperature / High Power Cells for Pulse Power

I.Summary

The lithium (alloy) / cobalt disulfide (Li-alloy / CoS_2) electrochemistry is currently under development at Westinghouse as a high power, pulsed energy source for mobile electric weaponry. Under ARDEC contract DAAA21-88-C-0029, a baseline 100 MJ, 2.1 MW pulse power system is scheduled to be delivered in the 1993-94 time frame. This fully integrated system consists of 40 bipolar modules, each employing 150 cells (150-200 cm^2 in active area), auxiliary heaters for activation and make-up of heat loss, a cooling system to remove waste heat, and a thermal enclosure to preserve the necessary operating temperature of 480-500 °C. Modeling studies indicate that this system will occupy ~0.40 m^3 and weigh approximately 855 kg. Baseline cells are 0.140 cm thick, consisting of positive electrodes designed to deliver an 80% depth of discharge based on 4/3 F/M (faradays per mole of CoS_2) with a 2:1 negative to positive capacity ratio. Cells are required to sustain a power density of ~1.73 W/cm^2 for twelve consecutive 4-second pulses (48 pulse-seconds, duty cycle ~80%, ie., 1 second rest time between pulses).

The goals of this LABCOM sponsored program were to optimize both cell components and operating conditions leading to:

- *at least a 10% reduction in system volume (to 0.36 m^3)*
- *a 100% increase in cycle life (from baseline goal of 100 cycles to 200 cycles)*

Volume reduction (as opposed to weight) was chosen as the primary objective since available volume is the controlling factor in mobile platform applications.

System level trade-off analyses were conducted quantify meaningful technical targets at the single cell level. These studies indicated that the volume of the power source could be reduced via two routes. One route was through an increase in power density, resulting in the use of fewer modules. A second route was through use of thinner cells. These two routes were independent and both were successfully pursued. Power density was increased to 1.92 W/cm^2 without loss of cycle life. Energy density was increased by designing cells for operation at 80% depth of discharge based on 1.75 F/M of CoS_2, a 30% increase in utilization, and by decreasing the negative to positive capacity ratio from 2:1 to 3:2, another 30% increase. These improvements can potentially reduce the 100 MJ baseline system volume by 10-20% if they can be successfully incorporated (individually or collectively) into multi-cell bipolar modules. Such multi-cell testing was beyond the scope of this LABCOM program. Improvements were transitioned to the ARDEC scale-up effort which focuses solely on multi-cell bipolar stacks.

Candidate cathode materials were investigated and only CoS_2 was identified as having excellent characteristics when operated in its higher voltage region. Alternate disulfides and chalcogenides could not match CoS_2 for pulse performance and open circuit stand capability.

Separator materials were investigated as replacements for the baseline Maglite D MgO. Silicon nitride, yttria, Magox Super Premium MgO and sintered, porous AlN were identified as suitable candidates for qualification as Maglite D replacements. The AlN was a dimensionally stable material and exhibited very low residual or final currents.

Cells were redesigned and tested based upon the above findings. The cycle life goal of 200 cycles was achieved with cells employing the reduced quantities of the active materials. The best cell tested exceeded 350 cycles and 2500 individual 4-second pulses. Freeze-thaw cycling was not a problem.

At the conclusion of this program, the potential for reducing the baseline 100 MJ system volume by 10% and increasing the cycle life to at least 200 cycles was reproducibly demonstrated with single cells.

II.Introduction

High temperature batteries are very attractive for meeting the requirements for volumetrically efficient, high energy, pulsed power sources associated with electric weaponry. At elevated temperatures chemical reactions are kinetically enhanced while the conductivity of ionic materials also increases. Salts in which the valency is ionic in nature are good conductors when melted. The halide salts of the alkali metals fit the requirements well and mixtures of such salts are responsible for freezing point depression so that mixed salts can have melting points in the range of 368 to 450°C. These temperature ranges are compatible with the lithium alloys and other active materials and components of construction comprising molten salt batteries.

The four major components of any battery system are the anode, cathode, separator and electrolyte. This program is directed to investigation of these critical components to develop a rechargeable battery cell capable of twelve 4-second pulses at a minimum power density of >1.73 watts/cm^2 and at least 200 charge / discharge cycles. As an organization, Westinghouse has been involved with secondary molten salt batteries employing an FeS cathode since the mid 1970's. The applicability of this lithium alloy/molten salt battery chemistry for electric vehicles has been demonstrated. This accomplishment spurred development of cells incorporating the highly reversible and thermally stable CoS_2 cathodes for higher temperature, higher power pulsed applications.

The thin plate CoS_2 bipolar battery has yielded over 400 kilojoules per kilogram (of cell weight) in pulse power testing using multiple pulses (up to 12 repetitive pulses at 1.2 A/cm^2 for four seconds duration) in multiple cycles (over 100) with multiple bipolar cells in series. These cells, weighing under 5 grams and having an area of 20 cm^2, delivered an average of 1.92 W/cm^2. This translates into a specific power of >4000 watts per pound and a specific energy of 50 watt-hours per pound. ***The specific power is approximately two orders of magnitude higher than aqueous room temperature batteries such as silver oxide-zinc. It is this extremely high specific power performance that makes this system viable as a pulse power energy source.***

This program has been carried out to support the ARDEC program (contract No. DAAA21-88-C-0029) and from time to time entered areas to solve questions or otherwise fill needs that arose within that program. The basic goals were to improve cell components and overall performance. These improvements were to be incorporated into the ARDEC program which will result in delivery of a 100 MJ, 0.40 m^3 system. This report covers all the work done under the LABCOM performance improvement and optimization program. It is divided into two parts. The first part deals with the cell components, consisting of the electrodes, electrolyte and separators. The second part deals with unit cells; their design, characteristics and handling. The focus of this development effort and the approaches taken are summarized in Table 1. The approaches followed directly from system level trade-off studies which quantified the sensitivity that the various cell fabrication and performance parameters have on the overall system volume.

III.Cell Components

A.Cathodes

The baseline cathode is CoS_2 and improvements were initially sought to replace first the transition metal cation, and later to replace the chalcogenide anion. Possible replacement cations are the other row 3 transition elements Fe and Ni as well as other multivalenced row 3 metals, Ti and V. FeS_2 is not stable at 480°C, the operating temperature of the Li halide electrolyte selected for use, and is ruled out for this investigation. Rows 4 and 5 elements such as Zr, Mo and W are interesting materials because two of them, ZrO_2 and MoS, are used in other nonaqueous systems with Li anodes.

The anion materials in the chalcogenide series are selenium and tellurium.

Table 1. LABCOM Development Goals Focus on Significant System Level Improvements

Objectives	Approaches
• Reduce 100 MJ baseline system volume by at least 10%	• Screen disulfide/ calcogenide cathode materials - Compare voltage/cycle performance to CoS_2 - Demonstrate pulse performance at 1.75 F/M MS_2 and Neg:Pos ratio of 1.5 (vs. 1.40 F/M and 2.0 respectively) - Demonstrate 12 pulse performance at 1.92 W/cm² (vs. 1.73 W/cm²) - Minimum end of pulsing voltage at >1.40 volts for good cycle life
• Replace Maglite D MgO baseline separator - Maximum allowable cell thickness = 0.140 cm - Final current < 5 mA/cm² at 100 cycles - Minimum end of pulsing voltage > 1.40 volts	• Obtain/test commercially available samples of MgO, Y_2O_3, Si_3N and AlN - Quantify performance and compare to Maglite D - Transition successful candidates into tape casting and 150 cm² cells - Verify performance in ARDEC bipolar stacks
• Demonstrate new, dimensionally stable separator concept • Qualify in 20 cm² test cells - transition to full size 200 cm² ARDEC cells if successful	• Obtain sintered, porous AlN - Fill pores with molten electrolyte - Fabricate and test cells - Evaluate performance
• Increase cycle life by 100% over present baseline conditions - 200 cycles - Maximum allowable cell thickness = 0.140 cm - Final current < 5mA/cm² - Minimum average power density = 1.73 W/cm² - 15 minute charge time for 6 pulse cycle, 30 minute charge time for 12 pulse cycle	• Quantify performance with both lithium rich and lithium poor anodes • Reduce recharge C.D. below 100 mA/cm² - Increase time of constant current charge and reduce time at constant potential - Quantify optimum charging parameters for maximum cycle life
• Characterize factors affecting cell-to-cell balance in high voltage bipolar cell stacks	• Leakage current analysis • Analytical model and seal requirements • Overcharge mechanisms • Cell electrochemical design via electrode states of charge and Neg:Pos ratio • Electrolyte management
• Support bipolar edge seal development - Quantify rate of underpotential deposition of lithium (on or in the edge seal) and its effect on cell life • Recommend acceptable materials of construction for bipolar edge seals	• Measure underpotential deposition currents with potential ceramic edge seal materials • Analyze the BN felt / LiF edge seals in used ARDEC modules and quantify the amount of elemental lithium present

These materials were tested by being made into pressed pellet cells. The cell electrochemical design was based on the assumption that the discharge capacity corresponds to two faradays per mole (F/M) of the oxidant. A mass of material was weighed so that the theoretical capacity was just about 0.4 Ah. After weighing, the material was admixed with electrolyte (20 w/o) and pelletized to make a 20 cm^2 disk. The corresponding anode was designed to have a capacity ratio of 2:1 using the $\alpha + \beta$ plateau region of the LiAl alloy. The typical anode mix contained 13 w/o LiSi alloy and 35% electrolyte. Finally, the separator was the Li halide mix (LiCl:LiBr:LiF) having a 440°C melting point and Maglite D MgO (approximately 50% by weight MgO and 50% by weight electrolyte).

The cells were fabricated under a dry argon atmosphere in a glove box located within a dry room and properly transported to another glove box for test in a controlled atmosphere. The test cells were mounted into a test stand. The test stand was a modified press having heated platens so that the cell could be heated to 480°C and held under a force of 35 kg. After reaching temperature and allowed to soak approximately 2.5 hours to reach equilibrium, the cells were top charged at 100 mA/cm^2 to a controlled potential, usually 1.95 volts. Pulse discharges were carried out for a 4 second duration at a constant current density of 1.2 A/cm^2. The discharge load was electronically applied and timed. Voltage and current data were acquired with a Nicolet 4049c Digital Oscilloscope and Nicolet XF44 dual disk drive, HP3497A Data Acquisition System and HP9817 for program control.

With the exception of NiS_2, the sulfides of Zr, Ti, W, Mo and V polarized severely although their open circuit voltages were high. Utilization of these materials was also less than that of the Co and Ni sulfides. Tungsten telluride delivered over 2.5 F/M in a two-step discharge at a current density of 0.77 A/cm^2, however, it could not handle the demands of the higher current density needed to achieve the target power density of >1.73 W/cm^2. Based on these results and calculations estimating capacity per unit weight, see Table 2, the work with other chalcogenides was shown to have lost its promise.

Table 2. Comparison of Molten Salt Chalcogenide Battery Materials with a Room Temperature Nickel-Cadmium Rechargeable Battery

Electrochemical Reaction	Formula Weight Sum	Gravimetric Capacity, mAh/g
$NiS_2 + 2\,Li \rightarrow NiS + Li_2S$	136.7	392
$3\,CoS_2 + 4\,Li \rightarrow Co_3S_4 + 2Li_2S$	396.9	270
$WTe_2 + 2\,Li \rightarrow WTe + Li_2Te$	451.5	119
$WSe_2 + 2\,Li \rightarrow WSe + Li_2Se$	355.7	151
$NiSe_2 + 2\,Li \rightarrow NiSe + Li_2Se$	216.6	247
$2\,NiOOH + Cd + H_2O \rightarrow 2\,Ni(OH)_2 + Cd(OH)_2$	331.8	162
$V_2S_3 + 2\,Li \rightarrow Li_2S + 2\,VS$	212	253

NiS_2 was investigated further because it behaved similarly to CoS_2. The major difference between the two seemed to be that while the initial 6 pulses had similar voltage levels, the NiS_2 electrodes had a steeper slope for the remaining 6 pulses. Low rate discharge of NiS_2 cells clearly showed three voltage levels, see Figure 1. The highest and lowest voltage levels coincided with the high and low levels of CoS_2, but the middle voltage level of the Ni sulfide was about 100 mV lower than the corresponding middle plateau of the Co sulfide compound. There was also a difference in the design between the two cells. It was known from the literature that CoS_2 had three voltage levels corresponding to the following reactions:

$$9\,CoS_2 + 12\,Li \rightarrow 3\,Co_3S_4 + 6\,Li_2S$$

$$3\,Co_3S_4 + 8\,Li \rightarrow Co_9S_8 + 4\,Li_2S$$

$$Co_9S_8 + 16\,Li \rightarrow 9\,Co + 8\,Li_2S.$$

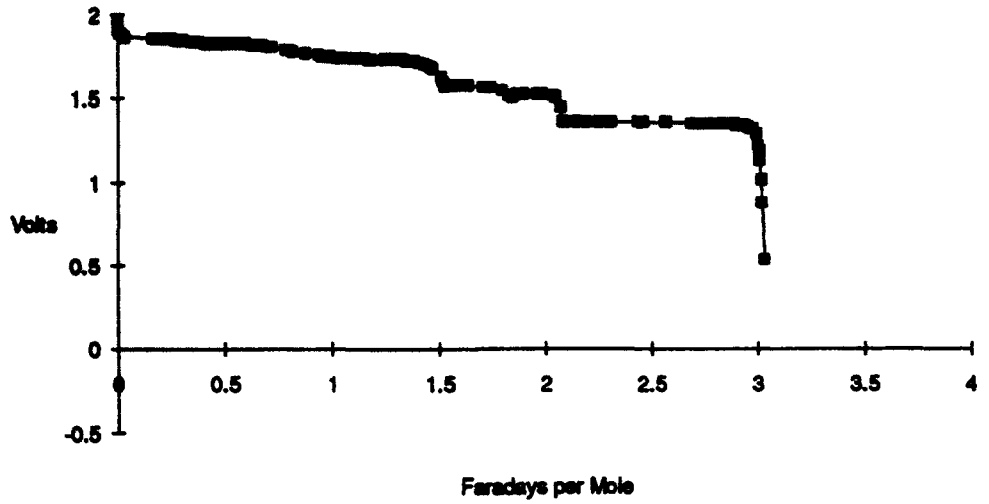

Figure 1. Nickel Disulfide Low Rate Discharge - Cell 2011 Cycle 32, J = 29 mA/sq.cm.

However, the prior literature revealed but two steps in the discharge of NiS_2. When both NiS_2 and CoS_2 cells are designed using the three observed levels in the discharge, then CoS_2 cells have a weight advantage, albeit a small difference but measurable.

The high rate discharges apparently cause the materials with the upper and middle voltage levels to discharge as a mixed potential. Since the NiS_2 middle voltage is 100 mV less than the middle level of the CoS_2 material, the mixed potential that of the NiS_2 material is correspondingly less than that of the CoS_2 material. When appropriately designed for a 4 F/M discharge the CoS_2 cell has a slightly greater energy density, and the effective impedance of the nickel compound is twice that of the cobalt compound:

$$V_{ecp\,Ni} = 1.663 - 0.0318p$$

$$V_{ecp\,Co} = 1.662 - 0.0152p$$

where p is the pulse number and V_{ecp} refers to the end of pulse voltage.

In the aqueous Ni/Cd battery doping the oxides of nickel with cobalt has beneficial effects and it was wondered if a similar synergy would be encountered if a small quantity of cobalt was added to nickel to make sulfides. At the 10% molar level there was some improvement but not enough to make the doping concept interesting.

The conclusion from this work is that CoS_2 is established as the best cathode material for very high power density pulse discharge applications. Other transition metal sulfides and other chalcogenides do not perform as well and also are heavier so that gravimetric energy densities are lower values than those associated with CoS_2. To minimize weight and volume for the ARDEC power source for electric weaponry CoS_2 as the cathode active material is the best choice of the materials tested. It should be mentioned that since NiS_2 and CoS_2 must be chemically synthesized (as opposed to naturally occurring FeS_2), the cost difference is not significant. As will be discussed in more detail later, the CoS_2 system exhibits excellent thermal stability with *virtually no self discharge on extended open circuit stand - even up to 8-hrs.* Based on these considerations, use of NiS_2 is not justified *at this time.*

B.Electrolyte Composition

An electrolyte in a battery cell must be ionically conductive. To have a good conductivity it must be operated at some temperature above its melting point. Its function is to participate in the charge transfer processes that occur at each electrode. Since the electrode processes are oxidation-reduction processes, the charge carrying process on the other side of the electrodes, the load side, are electronic in nature. These may be electrons or, equivalently, holes in the conductors. The anode process is the stripping of electrons from Li metal in the alloy resulting in electrons to the load and injection of Li^+ ion into the electrolyte:

$$Li(alloy) \rightarrow Li^+ + e^-$$

The cathode process removes a Li^+ ion from the electrolyte when an electron is captured from the external load:

$$3\ CoS_2 + 4\ Li^+ + 4\ e^- \rightarrow Co_3S_4 + 2\ Li_2S.$$

If the electrolyte consists of halide salts of different cations, eg., the LiCl:KCl eutectic (M.P. ~350 °C) there will be local compositional changes which can lead to precipitation because the local freezing points change accordingly. It is obvious that when only one cation specie is involved electrolyte composition is invariant. Transport properties, capillarity and gravity also keep the electrolyte in place. While the quantity of electrolyte is invariant the distribution will change because of compositional and density changes of the reactants and products which are related to the state of charge of the cell.

The electrolyte selected has the following composition:

LiF 22 m/o

LiCl 32 m/o

LiBr 47 m/o

This composition has a melting point of ~440°C. Typically, cells are operated 50°C above this melting point. Because electrode porosities change as a function of the state of charge, the amount of electrolyte installed into a new cell must be a quantity sufficient to avoid a capacity limitation to due a decrease of electrode/electrolyte interfacial area. The only way to determine this quantity at this time is empirically, and recounting of this work shall be delayed to another section of the report. Later we shall see that there is a "formation" of the cells, observed as an improvement of performance over the first 15-20 cycles. This improvement is associated with a change in thickness of the cell with time, and the redistribution of electrolyte. Electrolyte management is important in this as in other battery systems.

C.Anodes

The mixed Li alloys (LiAl, LiSi) were chosen to operate in the LiAl $\alpha + \beta$ plateau. This plateau ranges from an atomic composition between 10 and 48 a/o for LiAl. Also incorporated in the anode is a LiSi phase with an electrochemical potential close to that of the $\alpha + \beta$ phase transition. This operational region causes the anode to be 300 mV less anodic than pure Li, but this composition is chosen for several reasons. First is its ability to cycle between charge and discharge states. The second reason is that its melting point of approximately 640°C is compatible with the high operating temperatures needed to achieve high specific power and high electrode power densities. Power densities on the order of 1.73 watts/cm^2 (or preferably greater) are necessary to achieve practical packaged system volumes. In order to obtain information about regaining this 300 mV loss, a literature search was conducted.

Boukamp investigated conductive matrix alloys, but these materials have high polarization resistances. Huggins reexamined these alloys again in 1986 but no progress of significance to our work on pulse batteries was reported.

Liquid lithium anodes were the first kind looked at, but this required a material to confine the liquids and also required that the separating material be a fast lithium ion conductor. The so-called fast Li ion conductors known to date are only "moderately fast" and would not be suitable for the high rate/high power discharges of pulse batteries. There is a material composed of an ultrafine iron powder and lithium which is a paste above 200°C and can be formed to ingots. Catalyst Research Corporation (recently purchased by Saft), the company to which the patent is assigned, refers to this liquid anode as LAN. This material does have sufficient interest to be examined for the present application.

Argonne National Laboratory also had liquid anodes restrained by porous metal structures such as wicks, honeycombs, expanded metals, screens, foam metals and metal wools. The nature of the materials, Ni, Fe stainless steel were described by ANL. They obtained up to 70 charge-discharge cycles and that when failures did occur they were due to mechanical changes of the cathode such as swelling or movement. It should be noted that ANL used as electrolyte a eutectic composition of KCl and LiCl.

The failure modes of liquid lithium anodes were discussed by Vissers as well as Huggins[2]. These failure modes are an increasing impedance noted as increasing overvoltage, macroscopic shape change, operation below the melting point causing dendrites, filamentary or whisker growth which disconnect and gives rise to a capacity loss. Another major failure mode is deposition of Li which occurs everywhere the potential is appropriate and an electrode/electrolyte interface exists. In this case the solid electrode may be tab material or the collector material. The electrodeposition of pure metal can also cause a situation similar to supercooling which happens when there is solute depletion in the electrolyte. When there is a reaction of the electrode material with electrolyte and layers form on the electrode, these layers can ionically block further reaction. In turn the current density becomes nonuniform and cause local depletion of the electrolyte.

The above literature information had been used as a guide in the anode investigation. It is well-known that wherever the reactants are together and that a source or sink of electrons meet, and the Gibbs energy is negative, then the electrochemical reaction will proceed. Using these principles of heterogeneity and spontaneity we advocated that the cell case, if a conductor, not be at the potential of the anode. To achieve this it could be at a floating potential as when a feedthrough it used, or it may be at the potential of the positive electrode if this does not lead to corrosion, or an insulating film may be used to prevent the meeting of electrolyte and conductive case. A film of insulating material may be used to protect the tab and the internal terminal. Thus the electrode conductor, say an iron wool, in contact with the electrolyte is the only place where the conditions are appropriate for electrodeposition of Li.

Sources of porous anode bodies were sought. Steel wool manufactured by International Steel Wool Corporation in Springfield, Ohio, grade 0000 has a wire diameter of 0.015 to 0.025 mm having a composition of 11% carbon, 0.64 to 0.86% Mg, up to 3% sulfur and the difference being iron. The steel wool was cleaned using an alkaline cathodization. By compaction to a 90% porosity it is estimated than an electrode containing Li at 34 w/o should be our goal (the LAN has a composition of 20 w/o). The material was measured to determine whether it is adaptable on an electrode structural basis. The results were:

not compressed	1.52 mm	98.5% porous
slight compression	0.25 mm	91.1% porous
strongly compressed	0.13 mm	82.2% porous

The material appeared suitable with moderate compression. A holder was made to capture the material while impregnating with metallic lithium. There are two approaches for the impregnation. One is to rely on capillarity, and the second is via an electrodeposition process.

Steel wool which is mostly iron, was obtained locally in grade 0000 manufactured by Rhodes, was degreased and prepared by cathodization in 2 N NaOH solution. The material was cut to 5 by 14 cm,

weighed 2.791 g and was compacted to 0.625 mm in a frame fabricated in the model shop from stainless steel. The cathodization current was set at 2 amperes and run for 60 minutes. Weight loss on cathodization was 1.5%. As part of the cleansing technique after washing the steel wool to eliminate the NaOH, the remaining water was also eliminated using absolute methanol. The subsequent drying would allow rust to form if water is present. The cleaned steel wool was stored in a desiccator. The Harney patent[3] as well as the literature search revealed where Catalyst Research was investigating the use of Ni powders as a replacement for Fe in LAN electrodes. The search also revealed a Li_3N, Li composite termed Linode which is rechargeable and does not suffer the 300 mV loss caused by using the Al and Si alloys of Li. The rights to the Linode material are owned by the Canadian Government.

Other sources of structural anode materials contacted were EG&G Wakefield Engineering who could not meet the 90% porosity requirement and National Standard for Fibrex. All Fibrex made at present uses Ni and National Standard is not interested in making any from iron as a starting material.

While several of these materials have merit and the concepts should be pursued, our main objective was to provide timely support for the concurrent ARDEC program. For this reason this aspect of the program was not brought to a successful conclusion, and *the work deserves future support.*

D. Separators

The separator in use at the beginning of this program was Maglite D MgO, manufactured by Calgon/Merck. Because future supply of this material was questionable, it became imperative to find and qualify a substitute. Magnesia has many sources. Some sources are minerals dug out of mountains while another source is the ocean. The sources, its purification and the resultant particles somehow influence the acceptability of the MgO powder for use as a separator. Maglite D is characterized by being extremely low density and exhibits fluid-like properties.

The magnesia and electrolyte are mixed together in the required proportions and the composition allows us to refer to it as semidry. The entire cell may be considered semidry since there is very little or no mobile electrolyte in it when it reaches temperature. If too much electrolyte is used, the otherwise unbound separator washes out and the cell becomes shorted. The separator has no molecular bonding between particles and the powder is probably held in place by capillary forces.

Potential materials should be stable in the cell environment and these include ceramic type refractory oxides and nitrides. These include, of course, other magnesium oxide powders, titanium and yttrium oxides and among the nitrides are aluminum, lithium and silicon. One of these, AlN, has an excellent thermal conductivity and by means of powder techniques can be made into a porous sintered body. Sintering would then permit us to achieve a dimensionally stable separator.

1. Lithium Nitride

Lithium nitride (Li_3N) was dried overnight in a vacuum furnace at 350°C, sieved through a 300 mesh standard screen and made into a test cell. The material is maroon in the dry state and pink when admixed with electrolyte. Li_3N is a solid state ionic conductor with the Li^+ ion serving as the charge carrier. When the test cell was mounted in the test stand the cell exhibited a voltage of 1.1958 volts at 28°C. This is unusual since magnesia is an insulator and no voltage is read until the electrolyte is heated sufficiently to become an ionic conductor. Upon heating the voltage increased as the temperature increased. The cell reached a peak voltage of 1.806 volts when the temperature was 385°C, still below the melting point of the electrolyte. The voltage decreased first to about 1.6 volts and then to about 1.35 volts. The cell appeared to be self-discharging rapidly and when it fell below 1.2 volts charging was started at 100 mA/cm^2. The voltage went to 1.4 volts and then decayed while remaining on charge. The self-discharge rate appeared to become greater than the charge rate as evidenced by the decreasing voltage. The charging current density was progressively increased to 150, 200, 225 and 620 mA/cm^2 and at all levels the self-discharge rate appeared to be increasing. Upon charge interruption the voltage held at the 1.3 volt level for nearly two minutes and then fell to zero within another six minutes. This, too, appears similar

to discharge through an external load and suggests we consider the partial short circuit as an internal load.

The cell was inspected in the dry room. The pink color of the separator was gone although the three layers comprising the anode, cathode and separator could still be distinguished. The disk was fractured to aid observations and allowed us to discern that the edge appeared to have cobalt folded over. A piece of the disk of irregular shape was broken off so that the edge was no longer involved. The area of this piece is estimated at 0.8 cm^2. The resistance from face to face was measured using a Data Precision Model 2480 digital meter. The resistance is 0.023 kΩ using a two probe method.

The time at the various voltage levels are:

Upper	3.85 minutes	0.084 Ah
Middle	5.00 minutes	0.103 Ah
Lower	14.35 minutes	0.243 Ah.

These capacities were estimated from the resistance measurements (0.92 Ω for the 20 cm^2 cell), the voltage level and the duration. The capacity discharged sums to 0.43 Ah while the theoretical capacity for a complete discharge (4 F/M) is 1.23 Ah. The internal loss is three times this estimate. To reconcile this discrepancy we can assume the internal shorting resistance is not the 0.92 Ω measured at room temperature, but is about 0.3 Ω at elevated temperature.

The resistance may be regarded as having at least one non-blocking electrode and being made with direct current. The conducting species are electronic in nature and not ionic as required for the discharging process. The thermal coefficient of resistance showing a decrease with temperature augurs for something unusual as the conductor, not Al nor Co metals. This sort of behavior would be consistent with final currents being high and is, perhaps supplying some clue about the nature of final currents. Electrochemical systems to which a constant potential is applied have a current that decays to non-zero values. The processes that occur are generally called thermal reactions but may be due to shuttle mechanisms or due to interaction with the atmospheres. In multicell batteries which have no common electrolyte pathway shuttle mechanisms may be most important. It does appear that the cells of a series string of battery cells behave similarly for longer periods of time if the residual current is low. This similarity of behavior is expressed as "balance" or "matching" of cells, so that when a battery is placed on a constant current charge the cross-over point to constant potential is just about the same for all cells. When this occurs each cell undergoes discharge to the same depth and overcharge to the same degree. With low final currents the overcharge rates are equally low.

Upon cell assembly a voltage had been observed, and this is accounted for on the basis of Li_3N being an ionic conductor even at room temperature. We are dealing with an anode capable of producing Li^+ ions and electrons, a cathode capable of being reduced by ubiquitous Li^+ ions and electrons. All that is needed is a pathway for electrons to leave the anode and reach the cathode and such a pathway is supplied by the voltmeter. Upon heating to 385°C there is an onset of electronic conductivity directly between the anode and cathode. The electronic conduction increases with temperature and time.

The special conductivity of Li_3N is viewed as a detriment when used as a separator, but it still may be especially useful in the anode composition to attain the additional 250 to 300 mV per cell. In this case the electronic component of conductivity would be beneficial instead of detrimental to the cell.

2.Silicon Nitride Powders

Si_3N_4 was tested in cells using 2.0 grams of a 50-50 by weight mix of the powder and electrolyte. Si_3N_4 is an insulator and not an ionic conductor so no voltage is measured at room temperature. After heating to 480°C a top charge was applied using 1 ampere as a current limit and electronically limiting the applied

voltage to 1.95 volts. The input amounted to 14% of the theoretical capacity. It is known from XRD, DTA and other top charge work that the CoS_2 used is not fully charged, some Co_3S_4 being present resulting in about an 80% state of charge. The top charge serves to start the pulsing from a condition of full charge.

The end of pulse voltage on the sixth pulse was 1.58 V and on the twelfth pulse was 1.52 V on the very first cycle. After forming these values increased to over 1.60 V and 1.54 V respectively by the fifth cycle.

Si_3N_4 was considered a possible candidate for further qualification as a substitute for Maglite D.

3.Aluminum Nitride

AlN was tested as a powder as well as porous, sintered disks. The excellent thermal conductivity of AlN makes it very desirable as a separator since the thermal conductivity does not compromise its insulating properties. The powder materials do not lend themselves to fabrication of reliable separator pellets. In some instances the pellets broke, and in other instances the cells had some degree of internal short circuiting. Powder materials from two different sources, Alfa and Cerac, were used. The first step in overcoming these difficulties was to use greater weights of AlN (compared to baseline MgO separators), resulting in thicker, more robust separators less prone to damage or shorting. The materials from the two sources behaved differently. Unlike Cerac material, the Alfa AlN performed well in spite of the greater thickness. One cell exceeded 100 cycles with acceptable end of cycle voltages and demonstrated the chemical stability and physical characteristics necessary to qualify the use of AlN as a potential separator replacement for MgO.

To overcome the difficulties experienced with AlN as a loose powder, emphasis was placed on obtaining sintered disks of porous AlN. Based on their experience and expertise with AlN, Carborundum (Sanborn, New York) was selected to fabricate the porous bodies. Because the fabrication of thin (~0.025 in.), flat, porous AlN (35 - 50% porosity) had never been attempted before, it was decided to develop the process and test the strength, handling and operating characteristics with roughly 3 in. x 3 in. coupons. 2 in. diameter, 20 cm^2 discs could then be laser from these coupons and tested the same as all other 20 cm^2 cells used throughout this program. The decision to proceed with scale-up to full area (200 cm^2) pieces and incorporation into ARDEC test modules was dependent on successful concept verification at the 20 cm^2 size.

Note that the exact process used to produce these sintered AlN pieces is proprietary to Carborundum. Conceptually, the porous AlN samples are prepared by admixing AlN powder with pore formers and stabilizers and casting a green slab. The slabs are then sintered in a controlled atmosphere furnace. The pore former is decomposed in the furnace and the powder particles sinter about the openings left by the pore forming material. Porosity variations are obtained using different temperatures. The characteristics of three different runs are shown in Table 3. As can been seen, porosities can be controlled over a fairly wide range. The pore diameters and porosity were determined by mercury porosimetry. The strengths of the samples were inversely related to the porosities. Because of brittleness, these materials are best cut using a laser cutting tool in an inert atmosphere. A photograph of the disks and a micrograph showing the micro-structure are shown in Figures 2 and 3 respectively. All samples possessed sufficient strength to permit handling without breaking.

Table 3. Characteristics of Porous, 20 cm^2 AlN Disks

Sample	Porosity,%	Density, g/cm^3	Maximum Pore Size, u
V-115	48.6	1.72	0.32
V-120	42.2	1.93	0.29
V-116	34.8	2.18	0.27

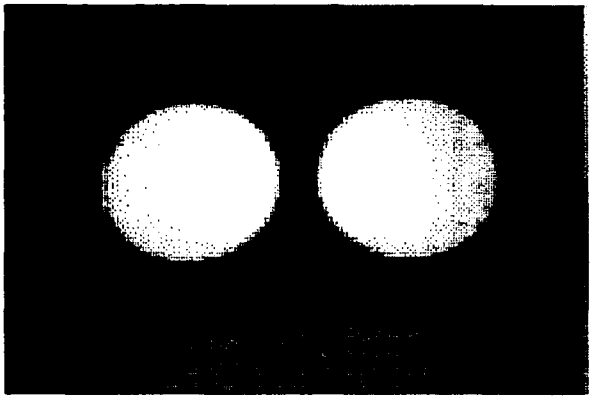

Figure 2. Fused separator laser cut to 2 in. diameter. Size is compatible with 20 cm2 test cells permitting testing of rigid, edge seal separator structures.

Figure 3. SEM photograph (x10,000) shows fused structure with open channel porosity. Sample shown is 35% porous - max. pore diameter = 0.27 μ.

These small capillaries have to be filled with electrolyte. This is an interesting process, first to get the molten electrolyte into the pores and second, to avoid distortion or cracking of the impregnated separator as the electrolyte cools and solidifies.

An aliquot of electrolyte was melted in a pyrex crystallizing dish inside a glove box containing a dry Ar atmosphere. The coupon of porous AlN was brought into contact with the melt at a very low angle to minimize gravitational effects and to prevent freezing as the melt ascends the capillaries. Capillary filling of this sort permits gases in the pores to be eliminated by replacement with the liquid electrolyte. Capillary filling did occur rapidly and the wetting front was clearly observed. Further, the 20 cm^2 disks remained flat and did not crack upon electrolyte freezing.

The thicknesses of these separators are 0.64 mm (0.025 in.) as compared to powder pressed MgO separators which are 0.2 mm thick (0.008 in.). Because of this, the end of pulse voltages are lower. The voltage limit on charge was increased from 1.95 volts to 1.98 volts to compensate for the greater ohmic drop in the separator. Pulse discharge testing consisted of five cycles of 6 pulses followed by a sixth cycle of 12 pulses (normal qualification routine). The results of the pulse performance are shown in Figure 4 for least and most porous of the AlN sintered separators along with a comparison to one of the better MgO powder separators. The MgO separator is about one third the thickness and has less of a voltage drop. Even so, these data do show that the average power does not suffer excessively from the use of the sintered AlN materials. System designs can compensate for the slightly reduced power levels; an average power density of 1.73 W/cm^2 over 12 pulses is the baseline point design for the 100 MJ (40 module) ARDEC battery system. While the power density values are deemed satisfactory, there are other aspects of these separator materials that are superior.

First, it should be noted that the data of Figure 4 are taken after the cells have reached the 100 cycles. Second, the final or background currents observed with the sintered AlN separators are the lowest values thus far observed, Figure 5. After formation, the 50% porous material yields background currents below 2 mA/cm^2 after charges of only one hour duration. Final currents decrease to 1 mA or less after overnight or prolonged charges. The less porous sinter has even lower background currents. The MgO material used for comparison has short term values of 5 mA which decreases to about 1 mA after the prolonged charges. There is some evidence that cells (in bipolar stacks) remain in better balance and cycle life is increased for cells with low background currents.

The thickness changes for these sintered AlN separators were compared with the powdered MgO separators. The thickness change over 100 cycles of the MgO containing cells is 0.25 mm (0.010 in.) while that of the AlN cells is only 0.15 mm (0.006 in.). It is felt that this difference is evidence that the sintered AlN separators are dimensionally stable. This dimensional stability augurs well for full size, 150

cell bipolar module design by reducing the cell stack collapse by approximately 0.60 in.

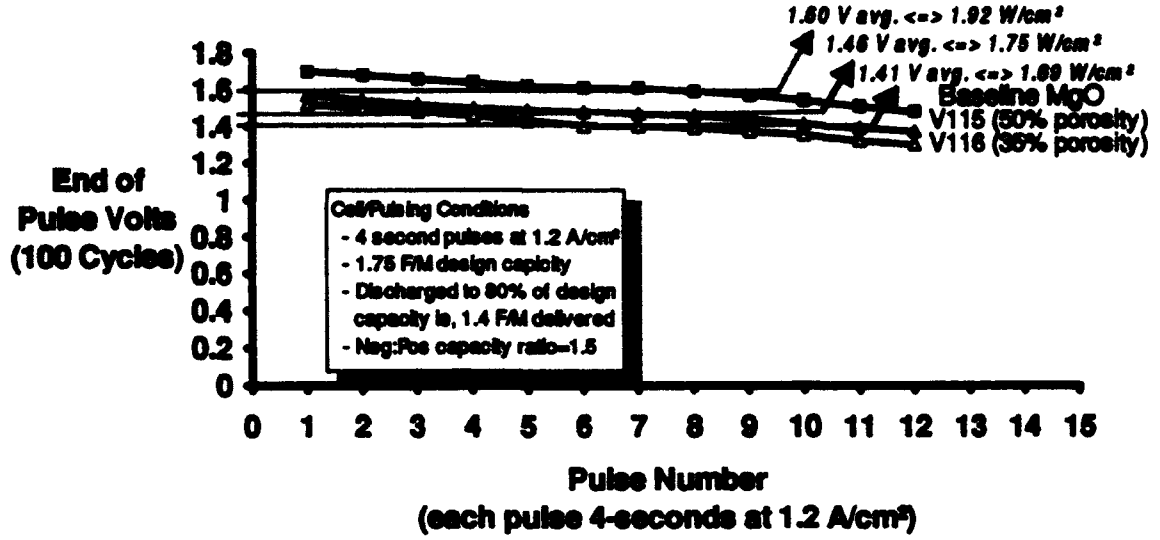

Figure 4. Both dimensionally stable AlN separators tested have exceeded the 100 cycle goal at average power densities which satisfy projected system requirements.

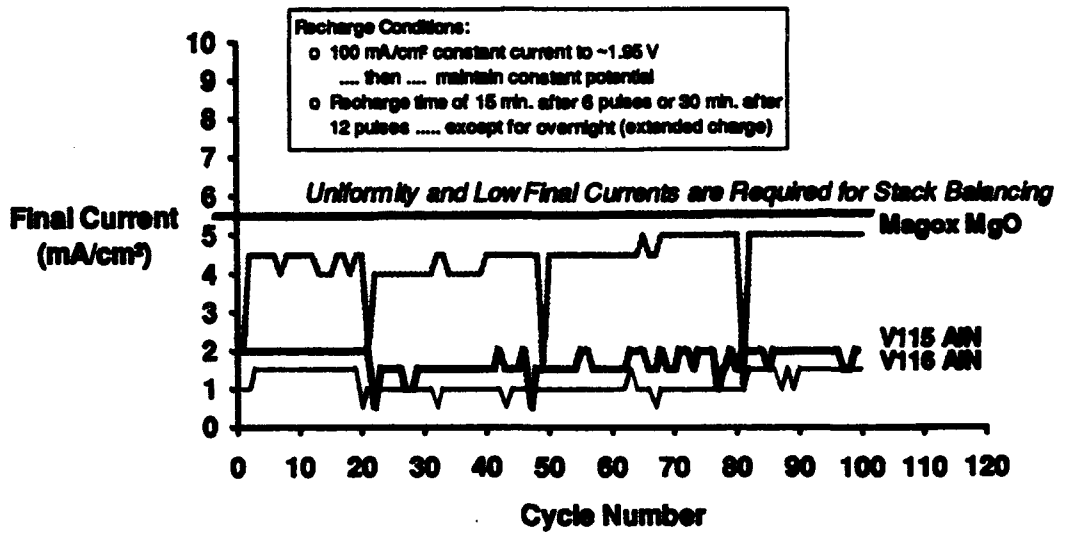

Figure 5. Fused AlN separators ranging from 35% - 50% porosity yield extremely low final currents.

There is also photographic evidence to support the contention that sintered AlN is dimensionally stable. Upon dissection at the end of testing the cells were fractured and examined. Micrographs of a V-116 separator (34.8% porosity) and of a MgO separator are shown in Figures 6 and 7. In addition to substantiating dimensional stability the AlN separator is pristine white as it was originally when the cell was made. There is penetration of the electrode materials into the MgO as evidenced by the discoloration, and the separator material was obviously compressed and distorted during testing.

Figure 6. MAGOX MgO separator after 372 cycles. Note banding in separator and "wavy" characteristic

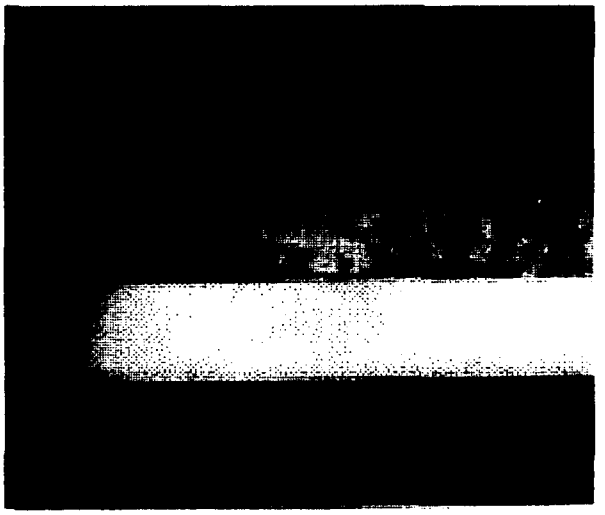

Figure 7. V116 AlN separator (35% porosity) after more than 100 cycles. Note pristine white color, complete absence of banding and the dimensional stability of the separator.

The surfaces of the sintered AlN separators were examined by heating the cell and removing the electrode pellets. The separators were found to have several cracks which led to testing for the freeze-thaw capability of this separator. Four freeze-thaw cycles were used. At the end of the test the cell was brought into the dry room for a cold resistance test with a digital ohmmeter which indicated the cold resistance was greater than 10 megohms. The test sample was heated and the cathode removed. Upon microscopic examination the separator was found to be cracked as were the first test cells and the fracture cross-sections were similarly clean and give yet more evidence of dimensional stability.

The low rate discharges of cells with the dimensionally stable AlN separators were informative. These discharges were carried out at 25 mA/cm^2 to minimize the ohmic loss due to the thicker separators. One such discharge is shown in Figure 8 where 856 mAh were obtained to 0.9 volt. This corresponds to 90% of the 4 F/M capacity (946 mAh). After an overnight recharge at 1.98 volts with a constant current limit of 100 mA/cm^2, the cell was subjected to 12 consecutive pulses under the standard 1.2 A/cm^2 for 4 seconds (320 mAh) followed by another 25 mA/cm^2 discharge, see Figure 9, and the total capacity obtained was 846 mAh. The end-of-pulse voltages were depressed by 100 mV when compared to values before the deep discharge, but the middle and lower plateaus were not affected by the deep discharge, neither voltage-wise nor capacity-wise.

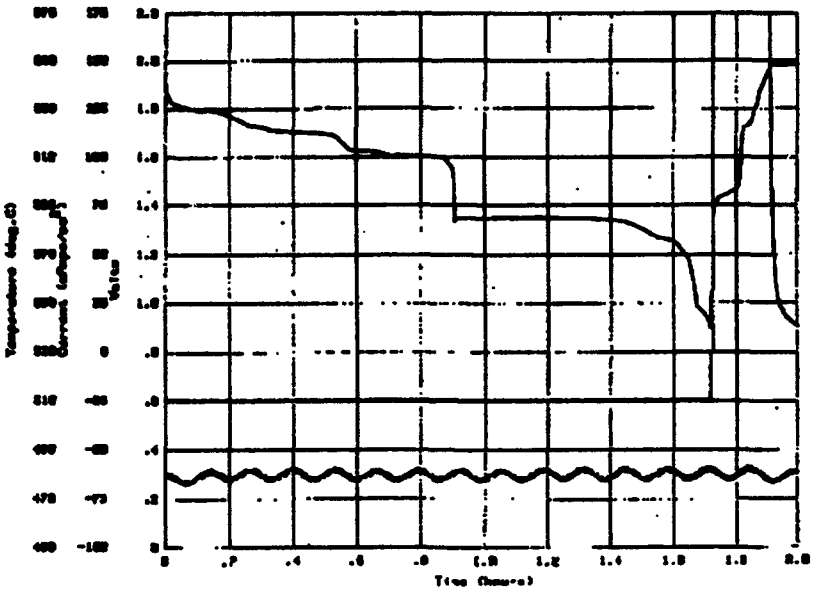

Figure 8. Low Rate Discharge of Cell LABCM2062F - Cycle 107

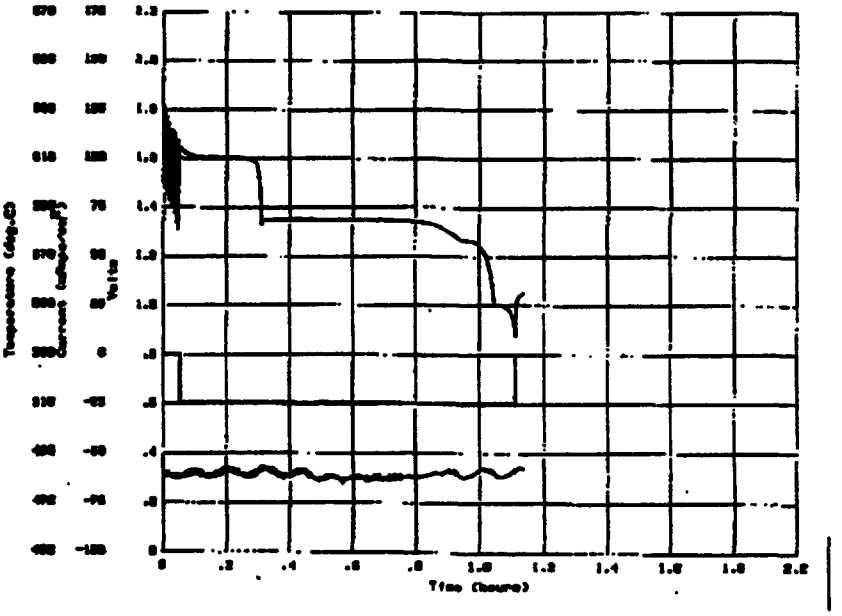

Figure 9. Cell LCBCM 2062F Cycles 106 to 110

In view of the quality of these test results it was recommended that larger separators suitable for use in future ARDEC test modules be fabricated. A photograph of a larger, 150 cm^2 separator is shown in Figure 10. Such pieces are laser cut (to the shape shown) from larger pieces that were of a square configuration. Scale-up to this size presented some problems. When heat treating to 500°C in the vacuum furnace a special effort was required to ensure that the work pieces were uniformly heated by the radiant energy to avoid a differential thermal expansion that would lead to distortion and fracturing. After solving this problem a special fixture had to be made to impregnate the larger separators. The metal frame holders used for the 5 cm diameter disks used thin wire, but similar frame holders of larger diameter wire introduced thermal shock and frames had to be made using the thinner wire. Also, the small angle used when inserting the separator into the molten electrolyte became critical with the larger pieces. Capillary rise in the pores is about 5 mm, and 5 mm for a 50 mm wide piece is less critical than 5 mm for a wider 150 mm separator. Now that the requirements for successfully scaling up the processes and procedures have been established it remains to qualify the larger separators using full size, tape cast cells in sealed modules.

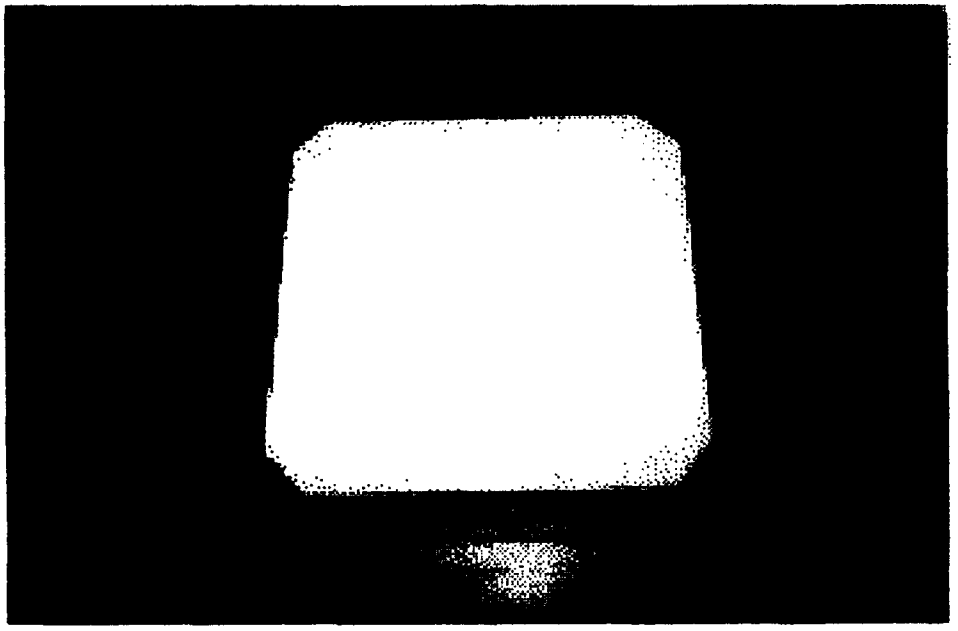

Figure 10. Full Size Dimensionally Stable AlN Separator

4.Yttria

Testing of yttria (Y_2O_3) was done using a mix of 58 w/o yttria with 42 w/o electrolyte and taking 2.4 g for the 20 cm^2 cell. The composition was selected on the basis of density of the materials so that the volume composition would be the same as the cells having MgO separators. The top charge insertion was in the order of 60 mAh which corresponds to 18% of the theoretical value of the CoS_2. This is in good agreement with the expected 80% state-of-charge as previously described in this report. The final current after the short term charge was 5 mA/cm^2. After several cycles, during which the formation process took place, the final short term charge current decreased to 3-4 mA/cm^2.

Pulse testing resulted in 1.54 volts at the end of the sixth pulse and 1.44 volts at the end of the twelfth pulse. After declaring this material as a candidate for replacing Maglite D, a cell with a yttria separator was stress tested. Stress testing involved a number of changes in procedures. Final currents were investigated as a function of charge voltage and these data are shown in Figure 11 where the 2.2 mA/cm^2 at 1.95 volts increased to 3.4 mA at 2.06 volts. We did not go higher in voltage because previous evidence indicated that some other process starts. The final currents were also followed to see how they

might change with cycle life or aging, but deep discharge cycles may have confounded the results. A number of deep discharges were run using the pulse discharge technique. On cycle 20 there were 19 pulses which resulted in discharge of materials at the upper and middle plateaus, followed by 37 pulses on the very next cycle to discharge all available material. This was subsequently followed by 34 pulses on cycle 28, and 39 pulses on cycle 52 . After the deep discharge on cycle 28, a degraded performance was observed. After leaving the middle plateau there is a loss of ability to recharge the cell so that the voltage levels on the upper plateau are degraded. Some of the degradation is overcome by prolonged charges, and from this we find that overcharge is beneficial to some degree and that the system appears immune to damage by extended overcharge provided the voltage does not exceed ~2.06 at 480°C. Some self discharge measurements were made which indicate that the rate is about 1% per hour, or one-tenth the final current.

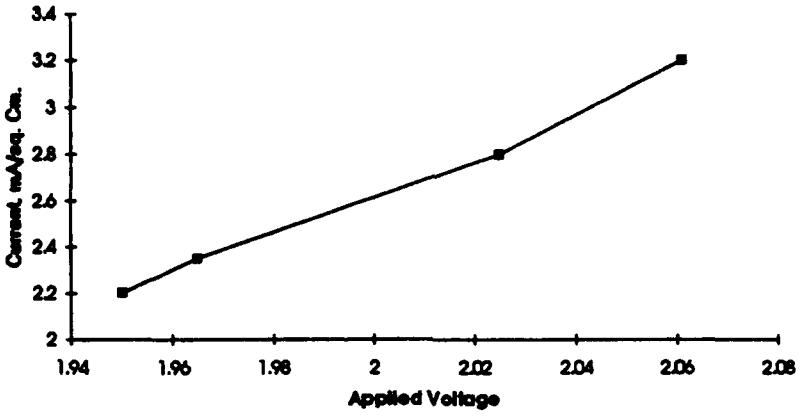

Figure 11. Final current - dependence on charge voltage

Duplicates not only verify the results but without the deep discharges the yttria separator system is able to reach and even exceed the initial goal of 100 cycles with end-of-pulse voltages of 1.63 volts on the sixth and 1.51 volts on the twelfth consecutive pulse.

One cell achieved 160 cycles before intentional shutdown. This cell incorporated the reduced quantities of active materials highlighted in Table 1 as being necessary to affect a significant 10% reduction in system volume. Stable power densities of 1.92 watts/cm² (also identified in Table 1 as a viable approach to reduce system volume by 10%) were maintained throughout the 160 cycles. At 160 cycles (approximately 10 days on-line), the final current had slowly risen to 5 mA/cm². Had this cell been allowed to run longer, it is clear from the pulsing data that it would have exceeded the 200 cycle goal established for this program.

5.Magnesium oxide

Three different kinds of MgO were tested. The other samples on hand did not possess an analysis or a set of physical properties that were similar to Maglite D. Tateho TA 152 and Elastomag 170 MgO materials were able to be pelletized and made into cells. However both of these failed to maintain a cell capable of being cycled since the cells became shorted for no obvious reason. There may be some electronically conducting aspect to these materials and interest was lost in them.

The third material subjected to test was obtained from Combustion Engineering's Premier Service Corporation and is identified as Magox Super Premium MgO. When mixed with electrolyte, the quantity weighed for use in 20 cm² cells had to be increased to 1.4 g (vs. as little as 0.8 g for Maglite D MgO) to avoid short circuits. The cell formed as expected and the voltages at the end of the sixth pulse were about 1.6 volts and at the end of the twelfth pulse are about 1.5 volts. Changes in performance show up

only later in life, see Figure 12, where it is demonstrated that even at cycle 331 the twelfth pulse had an end-of-pulse voltage of 1.4 volts.

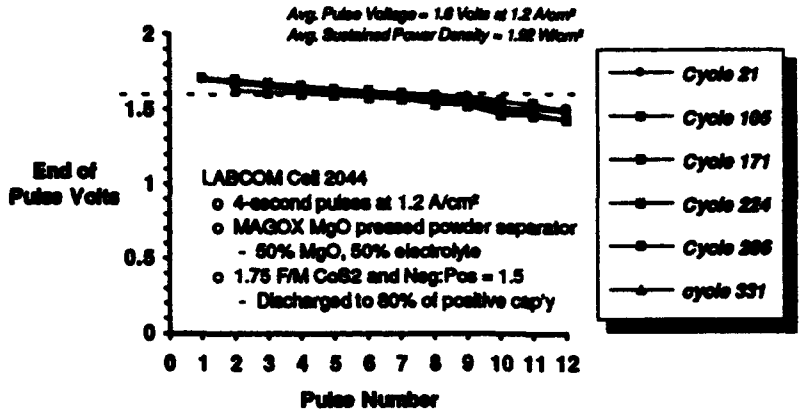

Figure 12. Stable Pulse Discharge Performance Has Been Demonstrated Over 350 Cycles and Nearly One Calendar Month of Operation.

The cycling was done manually during the day so that the charge continued during the night. The final currents recorded in the morning are shown in Figure 13. The extended charge resulted in currents of 2 mA/cm² or less for 372 cycles. At shutdown, this cell had logged 370 cycles and was maintained at 480°C for 25 days. The total number of pulses exceeded 2500.

Having exceeded the goal of 100 cycles so well, it was decided to experiment more with the cell. It was after 350 cycles that the current limit on charge was decreased from the standard 100 mA/cm² to 50, then 25 and finally to 10 mA/cm².

The cell characteristics also changed so that on the 25th morning of the test the final current had increased to 10 mA/cm² portending failure. The cell was stopped after 378 cycles. The cold resistance was 11 ohms indicating a short circuit existed that would leak about 10 mA/cm² agreeing with direct measurement. Final thickness was 1.0 mm indicating a shrinkage of 0.28 mm, also agreeing with the change in thickness obtained during the test with the transducer. The major thickness changed occurred over the first three days of testing.

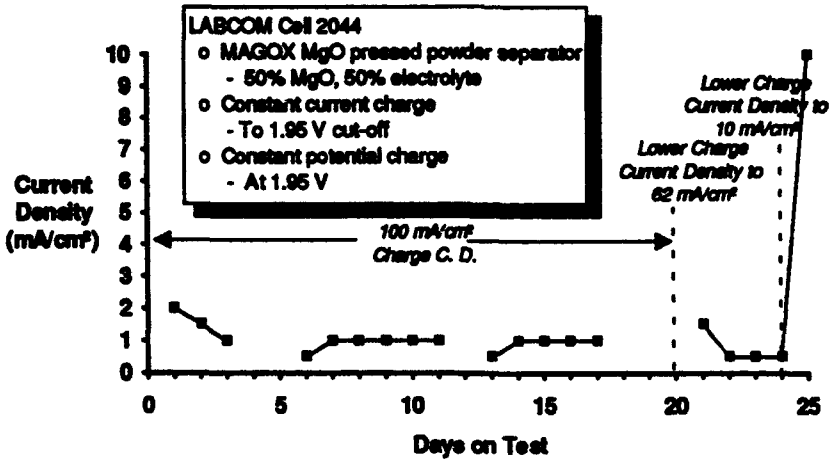

Figure 13. Stable Final Currents Have Been Maintained Over Extended Cycling. Rapid Cell Failure Occurred While Testing a Charge Current Density Below 50 mA/cm².

This test with decreasing current limits was considered confounded by the age of the cell since it had logged 350 cycles prior to changing the charge current density. Another cell was constructed using the same recipe. The first 16 cycles duplicated the previous results so that the charge current limit was decreased to 10 mA/cm². This change was applied on cycle 17 and by cycle 23 the final current increased to 23 mA/cm². Attempts to recondition the cell were futile. It was then inferred that decreasing current density below ~50 mA/cm² was detrimental to the system. This degradation does not show up immediately, but requires several cycles for the onset. The corollary of this inference is that the system is better behaved with the faster charges. This result has already been incorporated into ARDEC 20 and 50-cell module testing. Modules are normally charged at no lower than 50 mA/cm² to avoid this performance degradation phenomena. This lower bound on charge current density is used because it allows for safe recharge of the modules without overheating during recharge or extended overcharge (present 150 cm² module test configuration within the furnace does not incorporate any active cooling).

IV. Unit Cells

A. Test Cell Design

The base technology cells are made with commercially available CoS_2 which is dried in a vacuum furnace and then assayed for water content. This material has been analyzed by XRD and DTA and found to be typically 80% CoS_2 and 20% Co_3S_4. These analyses are in agreement with the top charge procedure adopted for evaluation testing of cells that indicate the material is about 80% charged initially. It had been thought that there are three voltage levels in the discharge of CoS_2 and that the uppermost level corresponds to the reaction:

$$3\,CoS_2 + 4\,Li \rightarrow Co_3S_4 + 2\,Li_2S$$

in which case there are 4/3 faradays of charge involved with each mole of CoS_2. Later we shall show that the upper and middle voltage levels discharge at a mixed potential and this was later used to make the cells thinner and lighter for the same kind of discharges. The initial design was based on this 4/3 F/M relationship and a negative to positive ratio of 2:1.

The 5 cm diameter cell has an area of 20 cm², and, historically, is built to a capacity of 0.4 Ah.

The cathode composition is :

CoS_2	76 w/o
Electrolyte (single cation)	20 w/o
Li_2S	4 w/o
Weight of Mix	1.89 g

The theoretical capacity based on 4/3 F/M is 0.417 Ah, and for a complete discharge to a value below Co metal production, 4 F/M, the theoretical capacity is 1.251 Ah. Since about 20% of the capacity is as Co_3S_4 the electrode must have sufficient Li_2S to allow the top charge to be effective:

$$Co_3S_4 + 2\,Li_2S \rightarrow 4\,Li + 3\,CoS_2$$

The amount of Li_2S required for the reaction to proceed without limitation is 71.3 mg and the amount built into the cell is 75.6 mg, a slight excess which should be sufficient to support the initial top charge.

The anodes should have an electrochemical design that provides sufficient capacity to discharge the cathodes, a reserve to accommodate the top charge and some charged reserve to accommodate some overdischarge. The anode composition is:

LiAl (17.5 w/o Li rich) alloy	52 w/o
LiSi alloy (19.8 w/o)	13 w/o
Electrolyte (single cation)	35 w/o
Weight of mix	2.2 g

A sketch diagramming the amount and distribution of the states of charge of the electrodes corresponding to the cell design is shown in Figure 14.

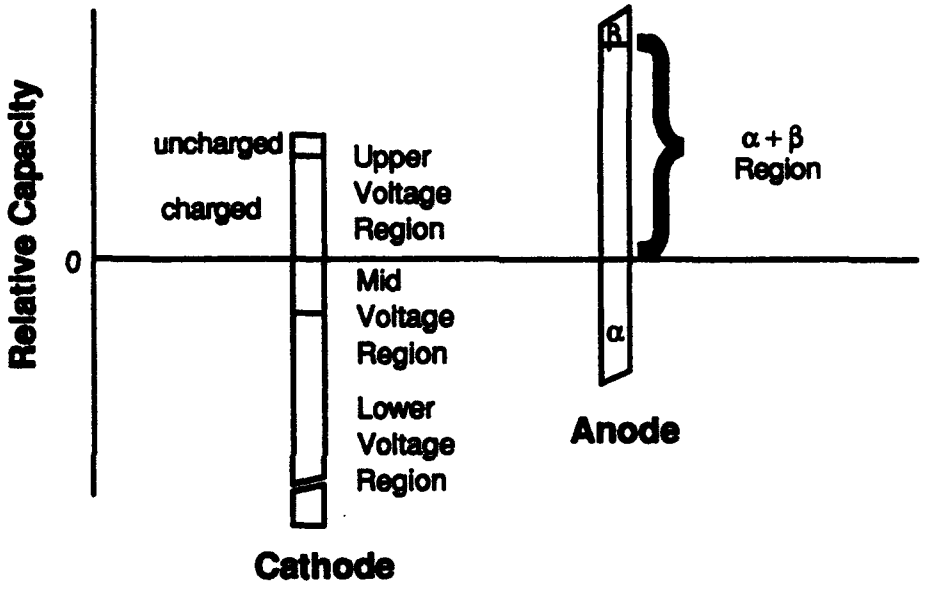

Figure 14. Cell Electrochemical Design

B.Utilization Improvement

Models for pulse power designs indicate that battery volume as well as weight densities could be improved by (1) operating the cathode at a deeper depth of discharge and (2) decreasing the ratio of negative to positive capacity. Such improvements should result in at least a 10% improvement in the volume of the ARDEC power supplies. There are indications in our previous work that it may be possible to operate the cell to a lower potential because the performance is that of a mixed potential during discharge. The caveat is not to completely discharge the middle plateau. We have been operating under the 4/3 F/M mode based on the upper plateau reaction:

$$2\,CoS_2 + 4\,Li \rightarrow Co_3S_4 + 2\,Li_2S\,,$$

and the assumption of a utilization of 80%. For a deeper depth of discharge the assumptions are changed to 1.75 F/M and the same 80% which is not unusual for electrochemical reactions.

A significant reduction of N:P ratio is going from 2:1 to 3:2. The state of charge of the anode was decreased to 90% by using material made to the corresponding composition on the $\alpha+\beta$ plateau. The initial testing for the increased depth of discharge was done by essentially not changing the design of the cell, but by increasing the depth of discharge. Sixteen pulses (vs. the usual 12) were run with the end-of-pulse voltage remaining about 1.4 volts.

Because a 90% state of charge LiAl alloy would discharge without involvement of LiSi alloy, the capacity computation for the anode mix did not include any LiSi contribution. The cell voltage is a little lower since the β phase was not entered to the exhaustion of the α phase material during charge. Because of this voltage lowering the charge voltage was also adjusted downward.

Later cells were redesigned decreasing the amount of cathode material to achieve just 12 pulses at a real F/M utilization of 1.4 (80% of 1.75) of the cathode material. The anode was weighed so that the Li capacity of the 10 a/o to 48 a/o Li in LiAl alloy is 1.5 times the CoS_2 capacity value. Both electrodes had less mass so that the weight and volume of the cells were significantly decreased.

These cells resulted in achieving 200 cycles with a minimum voltage of 1.5 volts on the twelfth pulse versus a target of 100 cycles with 1.4 volts minimum at the end of the twelfth pulse. Figure 15 shows the results of pulsing a cell with a deeper depth of discharge and a 3:2 anode/cathode ratio. The points are the individual pulses with the ordinate giving the end-of-pulse voltage and the abscissa presented in the F/M format. These results demonstrate the success of the thinner, lighter cathodes in achieving the required depth of discharge by yielding 1.5 volts at 1.4 F/M (actual delivered capacity). It was also found during the course of this work that the anodes at 90% state of charge discharge at about 20 mV less than those that are fully charged and termed "lithium rich".

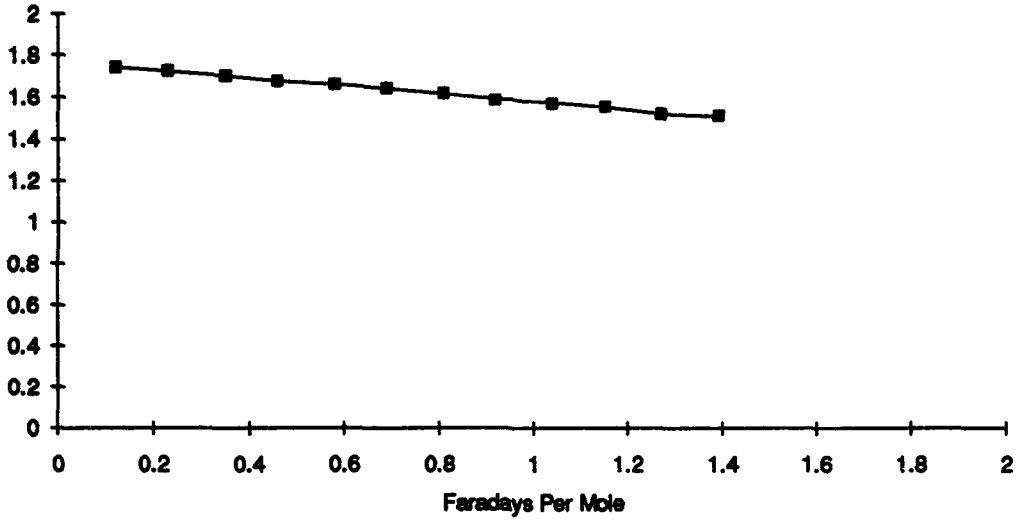

Figure 15. LABCOM cell 2037 1.75 F/M, "Li Rich", Pulse Discharge Cycle 177

Considering performance, final currents and cycle life, it is concluded that the Li rich anode material is preferable. Both types of anode accept the overcharge that accompanies a prolonged constant potential charge.

V.Reaction Entropy

The energy contained in a battery depends upon its reversible potential, E, and its capacity, and these are used to obtain the Gibbs Energy term,

$$-\Delta G = z\mathfrak{F}E .$$

In the discharge, capacity is withdrawn but the voltage is less than E. Let the voltage across the load be represented by V_T then the work done on the load by a current ι is ιV_T. The energy dissipated within the

battery is $\iota(E - V_T)$. Most batteries absorb energy from the ambient during charge, evident from cooling, and release an extra energy on discharge, evident by an extra heating. These are entropy exchanges with the ambient. This entropy term can be measured from :

$$\frac{\partial \Delta G}{\partial T} \equiv -\Delta S, \quad \text{and} \quad -\Delta G = z\,\mathfrak{F}E,$$

hence, $$\frac{\partial E}{\partial T} = \frac{\Delta S}{zF} \quad .$$

The open circuit voltage, E, is related to the Gibbs Energy term by the equation above. One of the values we need is ΔS to ascertain the entropy interchange with the environment.

On discharge the integrated current, $\int i\partial t$, can be no greater than the theoretical capacity. There can be a spontaneous discharge reaction that represent chemical decomposition or shuttle mechanisms or even reaction with the environment. Any of these parasitic reactions represent a rate of capacity loss, τ, which when multiplied by E represent the internal power dissipation. If we add to this the unaccounted for energy, $t\tau\iota(E - V_T)$. then the total power and energy are known. The thermal effect is to heat the battery. Next we need to know the heat capacity and the heat transfer rate to the environment.

On charge the problems become more confounded because the charge efficiencies are further from unity. Some fraction of the current goes into side reactions, the charge voltage exceeds the open circuit voltage or rest potential. The energy dissipated during charge consists of three parts:

entropy interchange with the environment.
$i_{parasitic}$ x total voltage.
$(i - i_{parasitic})$ x total voltage) - energy stored.

The sum of these values gives us the energy responsible for heat rise within the cell or battery.

To work out a model we again have two approaches of which one is heuristic and the other one is based on irreversible thermodynamics. Better yet, one may be regarded as phenomenological and the other as mechanistic. With the phenomenological approach we can surely fit the data, but lack insight. With a mechanistic approach good intuition is required to generate a model that does fit the data; this is the more difficult approach but the pay-off is more valuable. A successful mechanistic theory would enable an examination of the system for improvements. The discharge portion can follow the electrochemical model. The charge and overcharge process will require additional speculation on the processes, especially since we lack certainty in several regards. One area of unknowns concerns CoS_x where $x > 2$. We hope to identify other such areas during the treatment and penetrate them sufficiently to make an impact. In this way we may be able to treat charge and overcharge in a more quantitative way .

Entropy data come from the measurement of $\frac{\partial V}{\partial T}$. The cells being measured were adjusted to one of the three levels by charge or discharge. Data were taken during heat up as well as during cool down. The data were taken with a Keithley DMM 197 Autoranging Multimeter and temperature from the Hewlett-Packard Computer readout of the thermocouples on the test stand. Only the data from 420 to 480°C are used. The equation $V(T) = V(0) + \frac{\partial V}{\partial T} \times T$ was obtained from the data using the HP15C least square regression with the results shown in Table 4. From these values the entropy values are as follows:

Upper voltage plateau	28.8 calories per degree per mole
Middle voltage plateau	-26.8 calories per degree per mole
Lower voltage plateau	41.5 calories per degree per mole.

The entropy accompanying the middle voltage plateau is a negative value. The dimension of joules per mole per degree Kelvin is also known as the entropy unit. The entropy values enter the computer performance model (developed to predict transient electrochemical and thermal behavior) and influence the thermal aspects of module and multi-module system design. There are thermal changes during the pulse discharges and during the subsequent recharges due to the internal resistance of the system. In addition to the thermal generation there are the entropic changes. In this instance during charge at the upper voltage plateau, for example, the battery actually cools. This sort of behavior is not unique to this molten salt battery since cooling has also been observed as well in the room temperature nickel cadmium and silver zinc battery systems. So our thermodynamic measurements support the ARDEC mathematical model and are useful in the thermal design of modules and batteries made up from the modules.

Table 4. Thermochemical Data

	Plateau	V(0)	$\frac{\partial V}{\partial T}$	Correlation Coefficient	F/M
Thin Cells					
2084 heating	1.715	1.509	0.000278	0.972	4/3
2085 heating	1.715	1.498	0.000294	0.975	4/3
2085 cooling	1.715	1.521	0.000258	0.985	4/3
2088 cooling	1.370	1.314	0.0000745	0.996	16/9
Thick cell					
2087 heating	1.715	1.397	0.000432	0.964	4/3
Thin cell (no Si)					
2089 heating	1.715	1.549	0.000227	0.967	4/3
2089 cooling	1.370	1.137	0.000314	0.991	16/9
90%SOC (no Si)					
2124 heating	1.715	1.606	0.000234	0.9993	4/3
028S heating	1.717	1.6537	0.000132	0.999	4/3
028S cooling	1.35	1.2024	0.000336	1.000	16/9
029S heating	1.717	1.648	0.000143	0.998	4/3
029S cooling	1.63	1.735	-0.000211	0.999	8/9
029S heating	1.63	1.834	-0.000413	1.000	8/9

A. Final Currents

Electrochemical systems in a closed circuit condition do not usually balance out potentials, not even in potentiometers where a balance is struck by averaging settings. These small currents are referred to as thermal reactions and not investigated because they are considered negligible. We find that the charging potentials are associated with a current flow even after long periods on charge and these are termed final currents.

The speculation that final currents are due to leakage or self-discharge are not borne out by direct measurement of self-discharge. The measured self-discharge rate is an order of magnitude less than the final current. In the early stages of the work an expression was found for a cell which fit the following relationship:

$$\iota_f = 104x(V - 1.884)$$

where i_f is the final current density in milliamperes per cm^2 and V is the charging potential. The constants in this equation are believed to depend upon the nature and design of the cell. The design depending upon phases, states of charge, ratio of capacities, whereas the nature depends upon the specific chemicals used for the electrodes as well as depending upon the separator material.

As a cell ages the final currents tend to increase. This may be due to the cell becoming thinner or due to a material migration over the edge of the pellet (around the separator). Both of these do occur. Examination of the three-layered pellet structure reveals such edge migration. If the material that migrates is electronically conducting it is the equivalent of a short circuit.

There are two kinds of thickness changes. When a cell is first heated and tested, the molten electrolyte permits the particles to rearrange under the applied force. This is the initial large change discussed in the first part of this report in the section on dimensionally stable separators. There is another kind of change which is much smaller, shown in Figure 16, and deals with the state of charge. The cell becomes thinner on discharge and thickens again during charge. The dimensional change is dependent upon the state of charge. The thickness variation after 12 pulses show a delayed change at the start of charge and an overshoot in thickening on charge. As a result, the variation is thickness change is greater for the 12 pulse discharges than expected based on the 6 pulse discharges.

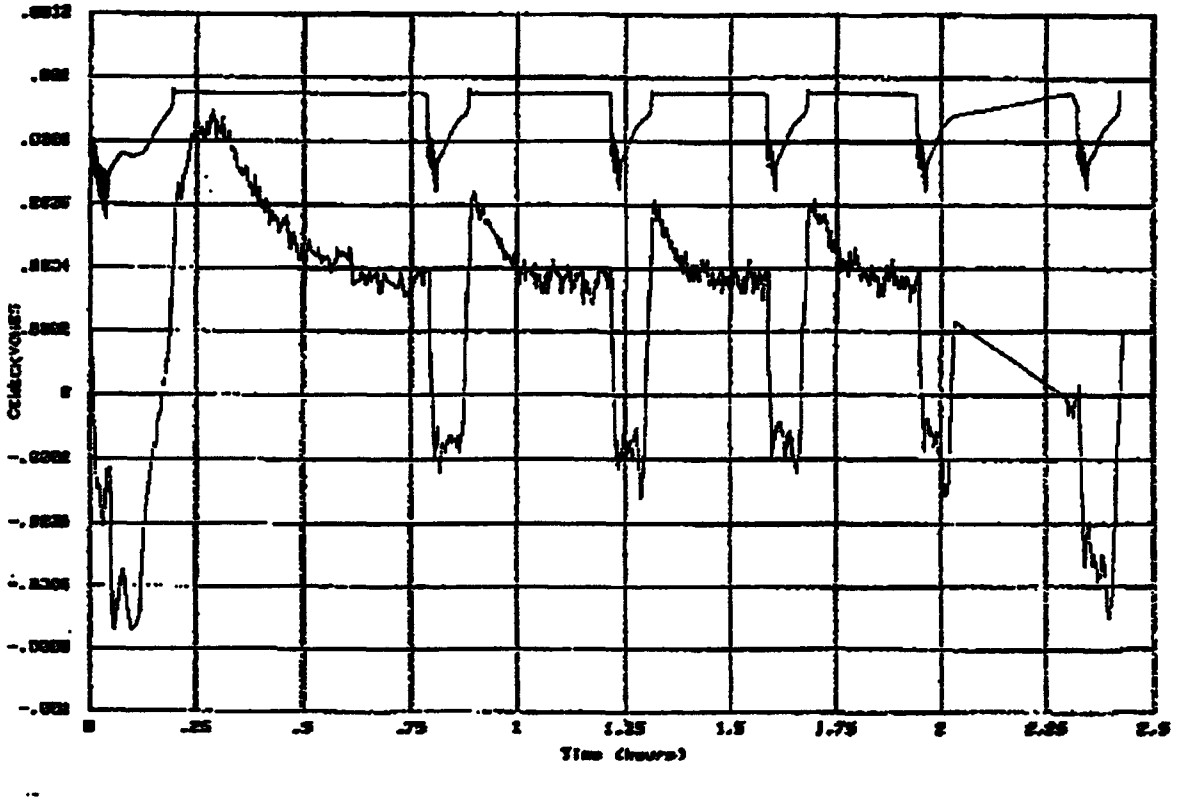

Figure 16. Cell LBCM2044H Cycles 203 to 210

The original goal had been to find materials and methods of construction to bring the final currents to values of 10 mA/cm^2 to decrease the failure rates. A number of separator materials were able to do this even though the cell design was more stressful. Figure 17 shows the effect of four different separators on the overnight charges in the design where the utilization of active materials was improved. The yttria and Alfa AlN powdered materials show the typical increase of final currents which occurs near the end of cycle life. The dimensionally stable AlN and Magox demonstrate the decreasing final currents as cycling proceeds. Along with this is also an improvement in pulse voltages. It is the set of these characteristics

that is considered as the forming process and is believed due to a redistribution of electrolyte.

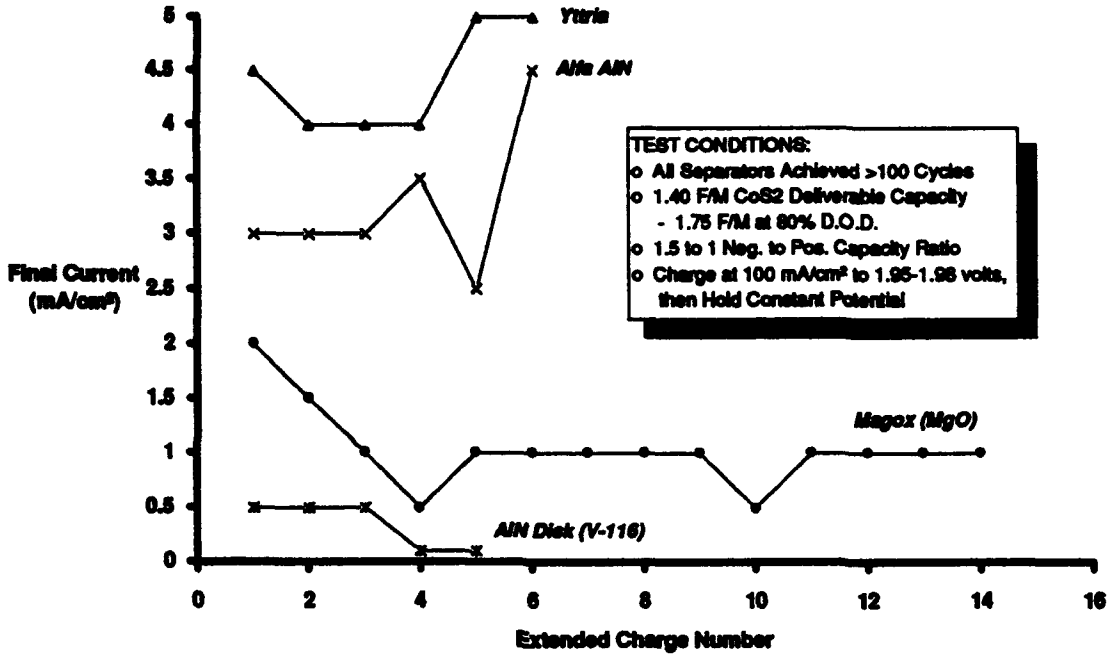

Figure 17. A dimensionally stable aluminum nitride separator achieved the 100 cycle goal with the lowest final currents measured to date.

As the final currents are decreased in value the cycle life of the batteries also is found to increase.

B. Rapid Formation

The building up or improvement in performance with cycling during the first 24 hours of testing has been recurring so that it appears to be a characteristic of the system. In other battery systems where formation is found such as lead acid, nickel-cadmium and silver-zinc there are combinations of treatments that accelerate formation. Since it may be either the cycling or the overnight charge that is responsible for the formation in the molten salt CoS_2/Li battery, the formation may be accelerated by applying the overnight charge in place of the top charge.

A cell with the new standard design, 1.75 F/M and 3:2 negative to positive ratio (Li rich) was heated and allowed to remain on charge overnight. The series of 12 pulses were then applied and it was obvious that a rapid formation process did not occur. After 5 sets of 6 pulses (five cycles) a second set of 12 pulses was applied on the sixth cycle. The end-of-pulse voltage data were improved. Apparently the charge-discharge cycling is needed to bring about the voltage improvement that we have termed formation.

C. Cell Balancing

There are a number of electrochemical factors that can influence final currents and cell balancing as well as several physical factors that can also affect cell balancing. Upon reaching an overcharge condition the electrode process changes and the electrolyte is decomposed. In the case of the positive electrode the overcharge conditions correspond to the complete conversion of Co_3S_4 to CoS_2, and yet current is forced through the cell necessitating a charge transfer reaction. A charge transfer reaction results in an external current. However, while oxidation occurs at one electrode, a coupled reductive charge transfer process

occurs at the other electrode. One possible reaction is oxidation of $S^{=}$ ion to $S_x^{=}$, a polysulfide. Similarly, in the case of the negative electrode where Li^{+} ion was reduced to Li_xAl until x=0.92, continued charge introduces a voltage increase from the mixed $\alpha+\beta$ plateau just to the β phase. The overcharge current is the "final current" in lead acid terminology and "leakage current" in molten salt terminology.

In addition to electrolysis the electrolyzed materials may be transported so that they meet in the space between the electrodes and react to reform the original material. Kaun describes a soluble Li that occurs with a slight increase of voltage, the polysulfides are also soluble in the molten electrolyte. When these materials recombine the salt, Li_2S, that had been electrolyzed is reformed. There are variations of this which may be achieved by design such as having an excess capacity built into one of the electrode so that the ratio of negative to positive capacity is not unity, and that the states of charge are such that one electrode reaches full charge before the other. As an example, consider a design starting with positive electrodes that contain Co only as CoS_2 and the negative electrodes with Li_xAl with x<0.92, but enough Li in the alloy to at least be stoichiometrically equal to the CoS_2 content. On charge this design favors $S^{=}$ oxidation before the negative electrode demonstrates a voltage rise corresponding to x exceeding 0.92.

There are mechaniams in some batteries which involve materials present in a cell which are reduced at one electrode, diffuse to the other electrode where they are oxidized and in this way cause a loss of charge of both electrodes. The S_x and Li mechanisms discussed above are similar to shuttle mechanisms but are confined to overcharge. Materials which can participate in an open circuit shuttle mechanism have yet to be identified.

Battery materials are chosen because they are very reactive - so reactive that they may decompose at a slow but finite rate. CoS_2 was found to decompose into Co_9S_8 and S, the sulfur pressure (and thereby the degree of decomposition) increasing with temperature. Also, Li does have some small solubility in the molten electrolyte. The dissolved Li that reacts with CoS_2 is replaced by material of the anode. Such decomposition and solubilization represent self-discharge which occurs on open circuit stand

The bipolar configuration permits cells to be closely packed, share cell walls, and combine the functions of wall and intercell connector. The many advantages of this configuration make it desirable, but the electrolyte of each cell in the battery must be confined within it. If there is electrolyte creep, and creeping is enhanced by the polarity, there may be encountered a pathway common to several cells. This common pathway gives rise to an intercell leakage current which alters the polarization and capacity of the electrodes in the battery. As a consequence, there is discharge which occurs as long as the common electrolyte path exists and between all those cells sharing the common electrolyte path.

There is always an ionic pathway between electrodes and any inadvertent electronic connection between the same electrodes completes the circuit. One way this can happen is by dendrite formation. The dendrites behave as whiskers and a very small point grows to touch the counter electrode, but the geometry is such that the effective resistance is high. This high impedance short can react electrochemically to break the circuit. The reformation and subsequent breaking or reaction of the dendrite gives rise to an intermittent partial short. The shorting can be made worse by the change in dimensions (volume) of the active materials as a function of the state-of-charge. The shorting causes some degree of discharge that would show up when leakage currents are measured, particularly during charge of the battery.

During the course of this development work there appeared to be a relationship between some of the experimental factors and the final current. We may discuss these factors but must note that a single mechanism may not be involved and the causes are confounded by interactions.

One of the factors that affect the magnitude of the final current is the composition of the anode. The LiAl alloys available early in the program had a composition more concentrated in Li than represented by $Li_{0.92}Al$. This material is termed Li rich and is entering the β alloy phase and potential range. If the alloy composition is maintained between 10 and 48 a/o Li the α and β phases are present and exhibit a constant potential 0.248 less negative than pure Li . A LiAl alloy maintained within this range where α and β coexist is, for convenience, termed Li poor. It has been established that the Li poor material is related

to cells having larger final currents than Li rich material and this is due to what may be explained as a difference in the back EMF.

The cathode material is not completely blameless with respect to final currents. Direct comparison of CoS_2 from Alfa and Cerac shows no difference in final currents. The CoS_2 material from Reed exhibits much greater leakage currents. The Reed material is physically different by flowing freely and being more crystalline in appearance.

Temperature also has an effect upon the final current, as may be expected. A plot of i_f versus T has a transition point at 425°C. Above this temperature the activation energy for the process is 4.52 kcal per mole and below 425°C the activation energy is 0.57 kcal per mole. The mechanism at the higher temperatures is probably a diffusion controlled process while at the lower temperatures the controlling mechanism is presumed to be electrical conduction.

MgO separators with calculated thicknesses of 0.2, 0.3, and 0.4 mm were built into cells and tested. The final currents were found to diminish as the thickness increased. There was an exception to this general observation - when the separator was made in two parts the final currents were lessened.

D.Effect of Non-Uniform Leakage Currents

In multicell bipolar testing the first few cycles indicate matched cells with respect to end-of- pulse voltages and end-of- charge voltages. Sometimes after the initial cycling the end of charge voltages diverge. Although the charge voltage limit applied is n x 1.95 volts, where n is the number of series cells in the battery, some cells reach values of over 2 volts and others are as low at 1.6 volts. This divergence subsequently results in poor pulse performance with the end-of-pulse voltages also diverging (due to some cells being insufficiently charged).

There are two observations made with these cells that help shed some light on the balancing or uniformity of behavior. These are: (1) the fact that they become thinner over the first few days of testing - *notably a reduction from 0.125 cm to 0.100 cm,* and (2) the movement of electrolyte from the core radially toward the edge of the bipolar wall.

In addition to these observations we have some knowledge that bears on the non-uniformity. One of these comes from the hermetically sealed nickel-cadmium cell field. With a great deal of effort to control electrode thickness, loading levels, separators and geometry of cell cases the void volumes of the core still varies from cell to cell. These void volumes are measured by electrolyte retention., If these cells can vary significantly, why not assume that the molten salt Li/CoS_2 can also vary from cell to cell. This means, then, that the electrolyte in some cells can creep radially to the edge of the bipolar wall. If a contiguous cell happens also to have excess electrolyte then the two films can meet and form an ionically conductive pathway between them. This situation is diagrammed in Figure 18 for a three cell bipolar battery. The electrolyte is shown as cross-hatched. The electrolyte between cells 1 and 2 is indicated as having migrated over the bipolar wall which acts as the current collector. This results in the anode of one cell and the cathode of the contiguous cell having two kinds of conductive paths. The electrolyte that has crept around the bipolar wall is an ionic conductor while the wall itself is an electronic conductor. The resistance of the wall is very small but the ionic conductivity of the leakage path depends upon the geometry of the thin film, path length and specific conductivity of the electrolyte. The current flow depends upon the impedance value of the electrolyte and the voltage difference between the cathode of cell 1, V_{c1}, and the anode of cell 2, V_{a2}, or:

$$j = (V_{c1} - V_{a2})/\Lambda ,$$

where Λ is the ionic impedance.

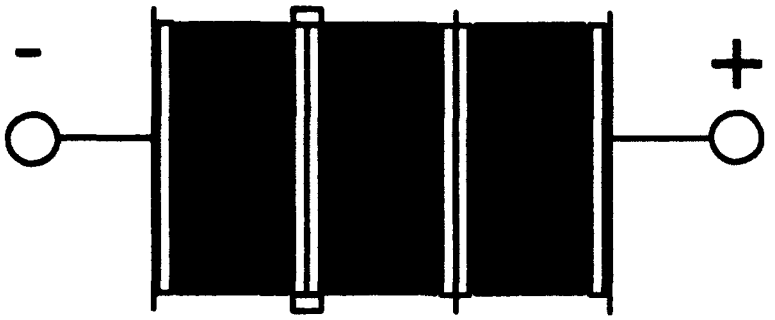

Figure 18. Stylized bipolar battery with non-uniform leakage path.

Note that the value of j depends upon the state of charge of the electrodes, but its sign does not change unless the battery is so deeply discharged resulting in a least one of the involved electrodes to change processes and cell polarity, an extreme condition. These contiguous electrodes, then, are always discharging whether the battery is being charged or discharged. If I is the charge current then electrodes V_{e1} and V_{e3} are charging at the rate I; similarly, electrodes V_{e2} and V_{e3} are also charging at rate I. Electrodes V_{e1} and V_{e2} are charging at a different rate equal to I - j. When the voltage limit is reached, the value of I decreases with time approaching the final current i_f. If i_f < j then electrodes V_{e1} and V_{e2} are discharging while the other 4 electrodes are charging or maintaining their states of charge.

Consider what happens when V_{e1} - V_{e2} = 1.6 volts corresponding to the middle voltage plateau and the battery is on a constant potential of 5.85 volts. The other two pair of electrodes are subjected to an effective 4.25 volts. Cell 3 has one pair of antipodes and its tap voltage will be measured as 2.125 volts. Cells 1 and 2 are confounded averaging 1.863 volts, but in reality one of the cells will be greater than this value and the other lower because the polarization of anodes and cathodes differ. Thus, the three cells will exhibit three different tap voltages. Pulse performance will obviously depend on state of charge of each electrode in the battery.

E.Open Circuit Stand

After charge a cell was placed on open circuit and allowed to undergo self discharge for one hour. The cell was then subjected to a set of 12 pulses. It was then returned to routine cycling for a number of cycles and again placed on open circuit stand, then, for two hours after 32 cycles. Following the same routine a four hour self-discharge period was allowed after cycle 40 and an eight hour self-discharge stand after cycle 48. The pulse performances are shown in Figure 19. In spite of the high temperature the rate of performance loss is not great up to four hours on open circuit. After self discharging for eight hours the system was able to sustain 10 pulses without significant performance loss. Even the last two pulses of the series remained above 1 volt. This kind of performance for a tetravalent transition metal chalcogenide in a molten salt battery system is noteworthy. Indeed, there is a military significance to these findings. This sort of electrochemistry can be extended to thermal batteries that have improved life and higher power capabilities, and can, therefore, be used for other applications such as sonobuoys. This extended open circuit stand capability of CoS_2 is in direct contrast to the performance observed with

FeS_2 which self-discharges considerably over much shorter time frames.

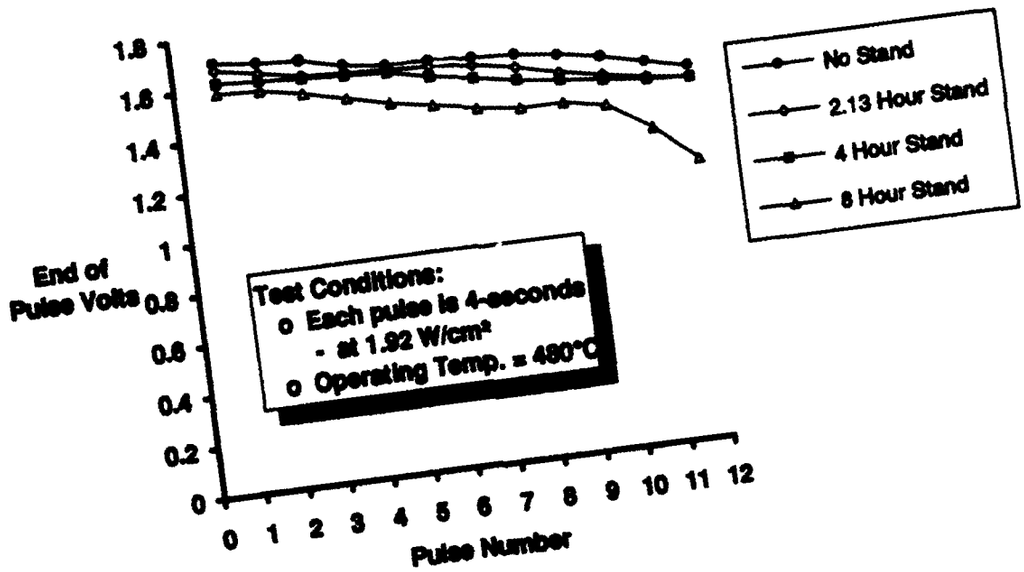

Figure 19. 20 cm² Cells Experience No Significant Loss of Voltage or Capacity After 8 Hours at Open Circuit

F.Charge Rate Effects

The standard method of charge has been to apply a constant potential with a current limit. The current limit has been 100 mA/cm² with 1.95 volts. It was determined earlier that we can raise the potential up to 2.04 volts with no adverse effects, but the effect of changing the current limit was of interest for several reasons. The first was to see if the total charge time could be reduced to 10 minutes and for this we set a higher current limit. The second reason is the capability of the charger, because as the cells are scaled up in area, the chargers similarly increase is size, cost and complexity with the consequence that there is an interest also in lower charge current densities.

At 200 mA/cm² the cell accepted the current very nicely reaching the cross over point to constant potential at a slightly greater ampere-hour input than at 100 mA/cm². When the charge current density was decreased below 50 mA/cm² the cells failed within just a few cycles. The failure is evidenced by an increase in the final current. This phenomenon is shown in Figure 20 ./here the final current is shown as a function of the surge current density. Too low a current limit is detrimental and the lower limit is thereby set at 50 mA/cm². An upper limit to the charge current density has not been approached experimentally. As the charge current is increased, it impacts the size, weight and cost of the charger. Furthermore, the joule heating encountered increases as the square of the current and the real upper limit in bipolar stacks may be set by thermal management considerations, not by the individual cells' ability to tolerate higher rate charge.

G.Electrolyte Management

When the cells become thinner during the initial testing some electrolyte is forced out of the cell. This creep is visible when used cells are examined, and, as discussed above, when the electrolyte from contiguous cells meet, an electrolyte leakage path is established which generates shunt currents and causes an imbalance in performance. This gives rise to the concept of electrolyte management in the

molten salt cells. There are two approaches that may be used. The first is to decrease the amount of electrolyte placed into the cell and the second is to employ an edge seal. Both of these approaches were investigated, and it may be pointed out that they are *not* mutually exclusive. This means that the two approaches may be used together, one to enhance the other and thereby improve the reliability for long-lived battery systems. Subsequent to this effort the ARDEC program encountered particle size and distribution differences from lot to lot of the separator material. In addition to this some differences of procedure with CoS_2 production were found. The particle sizes may contribute to electrolyte management, but we have not yet been able to conceive nor demonstrate how the CoS_2 contributes to electrolyte management, and this remains to be investigated.

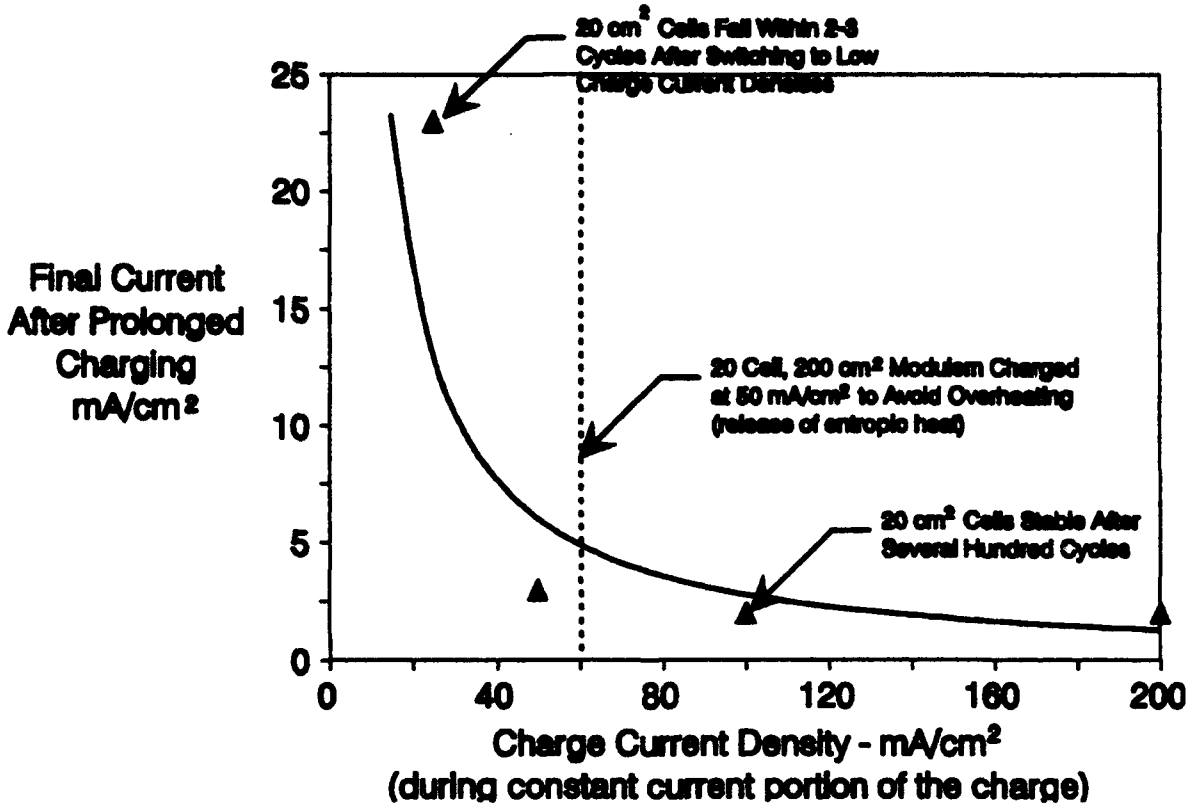

Figure 20. Charge Current Densities Below 50 mA/cm² Can Result in Rapid Cell Failure. Full Area Modules Must Have Sufficient Radial Heat Transfer Capability to Support this Charge Rate.

An amount of electrolyte was removed from the cell while in fabrication that corresponded to the 0.25 mm thickness change. There were several ways in which this reduction in electrolyte quantity could be instituted. In the first cell of the series the anode was prepared devoid of electrolyte and the amount in the separator was decreased. The next experiment prepared the three components (anode, cathode and separator) with only 38% of the usual quantity. The third kind of cell was prepared with no electrolyte in the cathode and a semidry separator. Thus these first cells all had but 38% of the usual amount of electrolyte but differently distributed among the three components.

While these cells were thin and lightweight, pulse behavior was poor even after allowing three days for formation. Over this period the performance improved, as expected, but not to the point of acceptability. Out of interest in performance at lower rates one of these cells (devoid of electrolyte in the cathode) was discharged at 100 mA/cm² to 0.9 volt. Capacity corresponded to 3.2 F/M. After a rest of 0.4 hour, at which time the voltage increased to 1.32 volts, the discharge was continued at 25 mA/cm² to 0.9 volt and the total capacity increased to 3.7 F/M, about 92% of the theoretical capacity. The effect upon power density capability is shown in Figure 21.

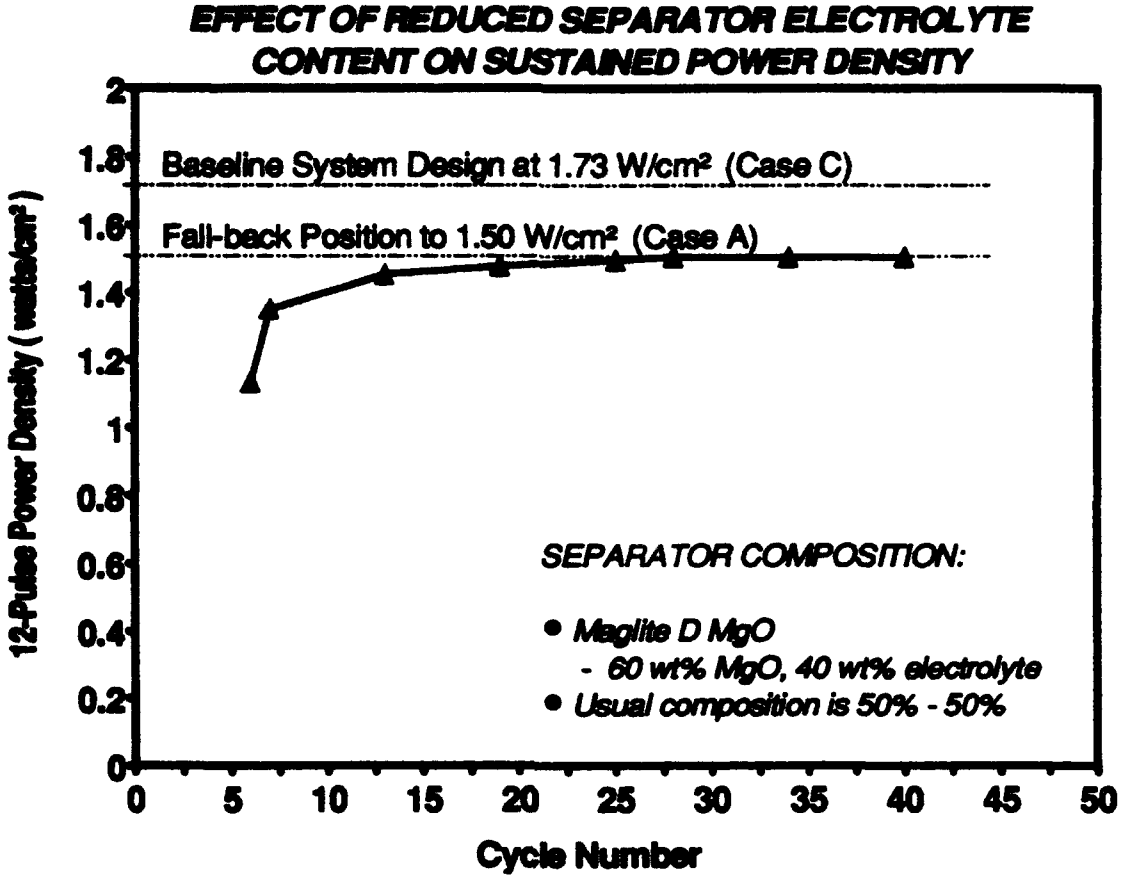

Figure 21. The electrolyte content of the separator can be reduced to 40%. Further reduction will result in unacceptably low power densities.

One conclusion drawn is that the amount of electrolyte removed was excessive. Second, the diminished electrolyte quantity meant that an electrolyte transport was needed to create the interface between solid and liquid for the charge transfer process. Hence, local current densities are high and voltages suffer. There is capacity present in these overly dry cells which is available at lower rates. At 25 mA/cm² we have obtained as much capacity as can reasonably be expected. Hence, we have to search for the proper amount of electrolyte and how it should be distributed within the cell. Recent ARDEC module experience suggest this to be an important piece of future work.

The next variation investigated involved use of the dimensionally stable AlN separator. Since the pores could be filled with molten electrolyte and the electrolyte content remains unchanged during heat up and compression we are able to decrease the number components being varied from three to two. Other work appeared to indicate that the electrolyte that leaves the pellet comes from the anode. Hence the cathode was standard using 20 w/o electrolyte. The anode composition was decreased from a standard 35 w/o electrolyte down to 19.5 w/o, but the amount of Li and alloys were unchanged. Testing results showed the formation phenomenon again whereby the performance improved with cycling. While 12 pulses were available, the voltages were low indicating a greater slope of the EOPV versus pulse number. From such data it was concluded that the optimum quantity of electrolyte in the anode lies between 19.5 w/o and 35 w/o.

The next experiment in the series incorporated an edge seal and the MgO electrolyte. The amount of electrolyte in the anode was decreased to 27w/o.On testing the cell required cycling as well as an overnight charge to undergo formation. Pulse discharge behavior was quite acceptable with background currents reaching 1 to 2 mA/cm^2, values considered as benign. The cell was given three prolonged charges including one that went a weekend. Examination after cooling revealed (1) a lesser quantity of electrolyte leaving the pellet and (2) a successful containment of that electrolyte which did leave the pellet.

VI.Underpotential Deposition of Lithium

Inside some bipolar cells in battery stacks of molten salt Li/CoS_2 there is elemental Li deposition. These deposits can build sufficiently to cause a short circuiting of a cell.

A similar Li deposition has been reported in ambient temperature non-aqueous lithium battery cells. Takeuchi and Thiebolt investigated this phenomenon in a single cell monopolar lithium/silver vanadium oxide systems. This is a primary battery and not rechargeable. When it is discharged the anode passes an electron to the external load and puts a Li^+ ion into the electrolyte. The cathode simultaneously accepts an electron from the external load which is used to reduce the vanadium and silver ion and takes a Li^+ ion from the solution. It is an insertion type electrode, frequently termed intercalation compounds. These workers used a stainless steel container hermetically sealed and having two, and in some cases three feed-throughs. Ammeters between the anode terminal and the case registered the Li deposition rate onto the case which was later confirmed by destructive analysis. They state that the configuration did not significantly differ from the standard case negative cells in performance nor the amount of Li deposited. The exact mechanism for Li deposition on the case was not given by these workers. They did infer that the deposition was related to the pulse discharge regime.

It was striking that the current flowed between the anode terminal and the stainless steel case, and that the authors were able to relate the total coulombic charge to the quantity of Li deposited. Ammeters are low impedance paths so that before the electrical connection was made the case was floating with regard to potential. Let us regard the cell container as an unpoised electrode while floating. When connected to the anode through the ammeter the following reactions are hypothesized:

anode: terminal metal / Li / electrolyte $\rightarrow e^- + Li^+$(electrolyte)

cathode: container / electrolyte (Li^+) + e^- $\rightarrow$ container / Li + electrolyte.

The electron is driven through the ammeter by the voltage difference of the two interfaces between solid and liquid. The anode has its well-defined potential by Li^0 / activity Li^+ ion in the electrolyte. The cell case, a cathode in this instance, has no defined potential being unpoised, changes its interface to approach the potential of the anode. As the potential changes the driving force lessens and the current decreases. The case is now regarded as a third electrode. When an ammeter is not present and the cell case is directly connected to the anode, the situation is essentially the same except that the ability to measure the current passing between the anode and the third electrode is absent.

The mechanism described above is not unique except for application to Li batteries whether they are molten salt or organic electrolyte batteries. It is a corrosion type reaction and we must recognize that this sort of mechanism has been used to explain rust formation, for hydrogen evolution, for adhydrodes, for supercapacitors and for other underpotential deposition phenomena.

The deposition of Li on the unpoised metal occurs at a potential less than that of the anode and, for convenience, we may call this mechanism the UPD hypothesis.

This hypothesis can be tested for application to the molten salt situation. A way conceived for testing the hypothesis is similar to that of Takeuchi and Thiebolt. A sketch of the apparatus is shown in Figure 22. An anode pellet is prepared along with a separator / electrolyte pellet. No cathode pellet is present. The two pellets are joined in the normal manner and mounted in the test stand. The anode is on bottom, its

usual position and it is on a normal collector, a Mo bipolar wall with a tab. A second collector, a tabbed Mo bipolar wall is slit as shown in Figure 22. The slitting is sufficient to ensure that when mounted as shown there is no electronic path between the tabbed side and the other. The Mo piece that is electronically floating is used as a control.

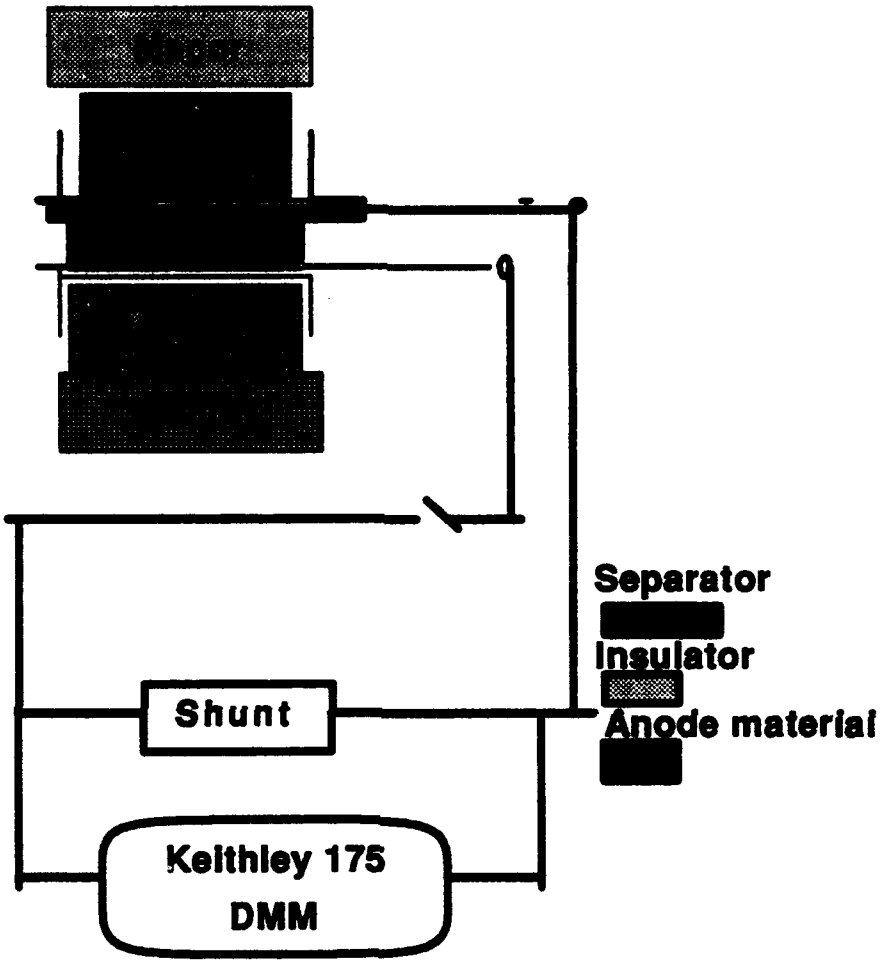

Figure 22. Test apparatus

The test stand is a converted press and has metal platens. these platens are insulated from the test cell by Macor insulators. The heaters surround the test cell and a Mo foil covers the heater. Hence, an insulator has to be placed over the Mo tabbed piece, which we refer to as "cathode", and the control piece or else these metal pieces would not be electronically isolated one from the other. The plan was to heat the test cell to 480°C, wait several days and then connect the two Mo tabs, but this connection should be through an ammeter or its equivalent. A two ohm precision resistor was used as the shunt and the Keithley DMM obtained the voltage drop and this is the equivalent ammeter. The voltage drop was also recorded using the data acquisition system.

It was intended to integrate the current-time relationship to obtain the charge passing between the two Mo pieces. At the end of the experiment the Mo cathode would be reacted with water and LiOH determined by titration with a standard HCl solution; this is the procedure used in reference 11.

The insulator in the first test using this apparatus was a ceramic BN disk. The current initially was 2.5 mA and this decayed to 180 μA in 55 hours. The shape of the current versus time curve was similar to that shown by Takeuchi and Thiebolt, but our currents were very much greater. Our final current is three times higher than their surge current.

Next the Mo "cathode" and its control were each leached in water and titrated for the alkalinity indicative of Li deposition. Coulometrically the amount of Li deposited was nearly 1 meq but the Mo "cathode" and the control each analyzed for 0.07 and .08 meq. Visually we saw the BN had swollen and discolored in the region where it was in direct contact with the separator, and there was a crack which had started at an edge and propagated along the junction between the Mo and the separator .

The BN was then leached in water and analyzed for Li. Its titre was 1.15 meq, greater than the coulometrically measured quantity. When investigated further it was found that BN hydrolyzes in water forming boric acid and ammonia and the ammonia affects alkalinity too. The previous data were corrected for the hydrolysis and the agreement between coulometry and titrimetry was good.

While the form of the lithium present in the BN is not known, we recognize that this experiment constitutes a procedure for testing high temperature insulators for our batteries. As part of this work the electrolyte salt was found to hydrolyze acidic, and when sheets of mica and AlN were leached in hot, agitated deionized water and the indicator added, the leachant solution gave no indication of basicity.

At the low level at which the Li specie is present in the ceramic and not finding conductivity it may be assumed that BN while not ideal may be used as an insulator in molten salt cells. The conductivity is determined with DC methods since this transport mode could be detrimental by causing a short circuit. Ionic conductivity would not be harmful since we already have such a conductor with the molten electrolyte.

VII.Testing Insulators as Edge Seal Materials

Having found a test procedure for evaluating insulators for the edge seals that help contain the electrolyte, it was applied to a number of materials. In each instance of testing the apparatus shown in Figure 22 was used, and the material to test was used as the upper insulator. From a plot of current versus time, the amount of charge passed between the two terminals is determined by integration. Figure 23 is a curve of current versus time for the apparatus with Coors AD99.5 alumina as the insulator. These are not typical data since the others start with a high current that decreases with time much like that of Takeuchi and Thiebolt.

In most instances the closed circuit experiment was carried out for about 55 hours. After cooling, the following components were separated and contained in a dry atmosphere: (1) the insulator, (2) the portion of the molybdenum collector which had been connected to the anode through the shunt, the "cathode", and (3) the portion of the collector that remained at open circuit conditions and is the control for the experiment. These three items were individually placed in water, stirred and heated and then titrated with HCl to a phenolphthalein end point. All results are converted to milliequivalents (meq) since 96500 coulombs are equal to 1000 meq by definition, and the product of volume in milliliters and HCl concentration in normality is also a meq term.

Before reviewing the results using 7 kinds of insulators, the possible reactions are considered.

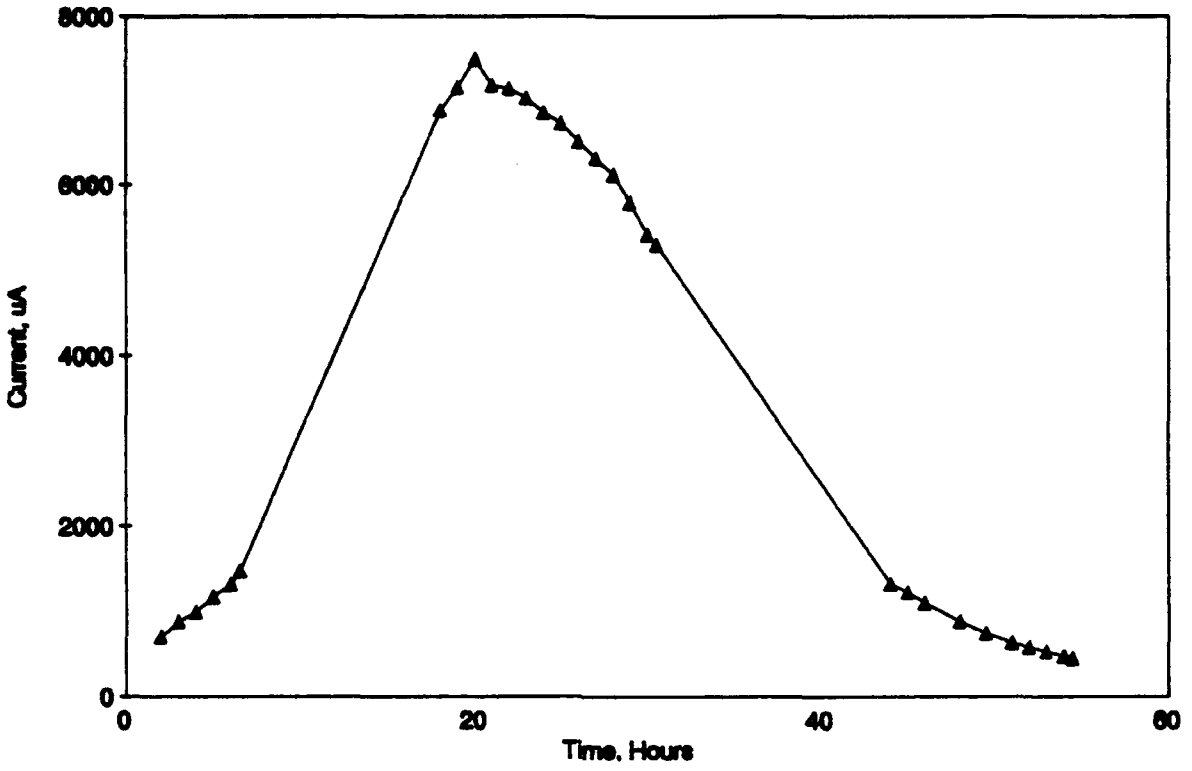

Figure 23. Underpotential Deposition Experiment with 99.5% Alumina

A. Review of Possible Reactions

There is no reason to expect only one mechanism to be involved when the circuit is closed on the apparatus of Figure 22. The processes thus far conceived are:

Underpotential deposition
Ion Exchange
Shuttle mechanisms
Diffusion
Chemical (metathetic) reactions.
Intercalation.

The current and its duration is of such magnitude that it can not be ignored. The current is the rate at which some material is oxidized at the anode which is exactly equalled by some reduction process at the cathode. These coupled reactions occur by charge transfer processes at the respective interfaces which we shall examine now.

1. Underpotential Deposition

The anode interface consists of molten electrolyte and the solid Li alloys. The potential is governed, in part, by the oxidation of Li to Li^+ ion, as we know from other experiments. The potentials for the oxidizable materials which are identified are:

$Li \rightarrow Li^+ + e^-$ -3.05 volts

$Al \rightarrow Al^{+3} + 3\,e^-$ -1.66 volts

$Si + 4\,F^- \rightarrow SiF_4 + 4\,e^-$ -1.2 volts

$3\,I^- \rightarrow I_3^- + 2\,e^-$ +0.54 volts

The Li/Li$^+$ potential is sufficiently negative to maintain the other species in the reduced form. These considerations should be sufficient to establish that the anodic process is Li oxidation.

The coupled cathode process is more difficult to identify since the "cell" was not built with a readily reducible material. The molybdenum is already reduced. The halides are also reduced. One of the materials tested was a cast, fired LiF board. It is only the Li$^+$ ion of this material and of the electrolyte that is reducible. In which case we may write:

$$Li^+ + e^- \rightarrow Li$$

and this is, therefore, an underpotential deposition and the half cell may be written as:

$$Li^+X^- \;//\; Li,Mo$$

The Li deposited upon Mo may diffuse into the structure of the LiF. As part of the experimental work it was shown (1) that the titre for LiX electrolyte is zero, and (2) that a control board of treated, cast LiF also had a zero titre. If these reactions are combined to characterize a complete electrochemical system, the following is obtained:

$$Mo \;/\; Li(Al,Si) \;//\; Li^+X^- \;//\; Li \;/\; Mo$$

a system analogous to other underpotential processes such as hydrogen adsorption in supercapacitors, lead on gold and the adhydrode.

2. Ion Exchange

Mica being chemically similar to vermiculite may undergo ion exchange reactions as evidenced by the work of Maraqah and his coworkers. A heavier metallic ion in the mica structure, such as K$^+$ and Mg^{++} ions may undergo an ion exchange reaction with the molten electrolyte. When placed in water for leaching, the protons of water would then exchange with the Li$^+$ ions, i.e.,

$$Li^+ + K^+\text{-mica} \rightarrow K^+ + Li^+\text{-mica}$$

$$Li^+\text{-mica} + H_2O \rightarrow LiOH + H^+\text{-mica}$$

The leachant becomes alkaline and is titratable. In this way an alkalinity greater than that equivalent measured by coulometry can be encountered.

3. Shuttle Mechanisms

One of the overcharge shuttle mechanisms promulgated at ANL is rewritten as follows:

- negative interface

  $Li^+ + e^- \rightarrow Li$ charge

  $Li + Li^+ \rightarrow Li_2^+$ dissolution

- positive interface

  $Li_2^+ \rightarrow 2\,Li^+ + e^-$ discharge

When these are added together, there is no net reaction which is indicative of an effective shuttle mechanism. In the event of a shuttle mechanism operating we would have to find a lesser quantity of Li metal at the "cathode" region than indicated by coulometry.

4.

4. Diffusion

A lithium diffusion process may not be stand alone, but accompany other processes. Thus lithium as the element dissolves in the electrolyte from the anode and diffuses away from the source. Nature tends to make the solution uniform in concentration. When the dissolved, elemental Li reaches the "cathode", nothing further is expected to happen since there is nothing reducible.

If Li can enter the structure of the insulator, then a diffusional gradient is set up and deposition at the insulator continues. In such a case the quantity of Li found by analytical techniques can exceed that measured coulometrically. In this instance, as differing from ion exchange, the Li is metallic and behaves as does the metal when placed in water. If the metal is transported from the anode via a dissolution-diffusion process then titrimetry yields values greater than coulometry. If the transport is via UPD which is then followed by diffusion into the insulator, titrimetry and coulometry should yield the same values.

5. Metathetic Reactions

With simple metathetic reactions there is a similarity to the ion exchange reactions, except that a valence change is involved. Using alumina as an example, the metathetic process is:

$$6\,Li + Al_2O_3 \rightarrow 3\,Li_2O + 2\,Al.$$

The sort of process would result in two effects. The first is that upon subsequent treatment with hot water LiOH would form

$$Li_2O + H_2O \rightarrow 2\,LiOH,$$

and this would cause the titrimetric determination to exceed the coulometric measurement. The second result could be a discoloration of the alumina due either to the presence of Al particles or due to the introduction of defects into the structures of the Li-Al oxide structures.

MgO was not tested, but there is a possibility of an analogous metathetic reaction between elemental Li and magnesia.

6. Intercalation

Intercalated chemicals are those where some specie is integrated into the structure of the host compound. It most usually is accompanied by an oxidation-reduction process, however, that would not be the case in the capture of Li, but an important characteristic of the intercalation process is a volume change of the insulator.

If intercalation is involved the "cathode" molybdenum may not have any significant quantity of Li by titrimetry, but the insulator is swollen and may even have undergone a color change.

B.Experimental Results

While there were 6 possible reactions reviewed, there is a seventh type of happening which could arise. When separating the 3 components from the "cell" which has anodic material, there was an attempt to prevent cross contamination by avoiding any material easily removed from the molybdenum pieces or the insulator. Hence, errors may be introduced whereby less Li is titrated than measured coulometrically. In one particular instance it is reasonably certain that a very small lithium nodule was removed.

Seven materials were investigated. To analyze the data a plot was made of the difference between titrimetry and coulometry measurements versus the coulometric measurement, and it is shown as Figure 24. A horizontal line was drawn through the intercept zero. Values which lie near zero are consistent with an Underpotential Deposition (UPD) mechanism. The graph shows two of the seven values which differ

significantly from zero. The major negative deviation corresponds to the used mica samples and the second is a large positive deviation corresponding to the Coors AD94 alumina. In both instances the coulometric charge is quite high. While from a fundamental viewpoint the identification of the mechanisms responsible for the errors may be a source of satisfaction, such information would not be useful in designing a better battery component.

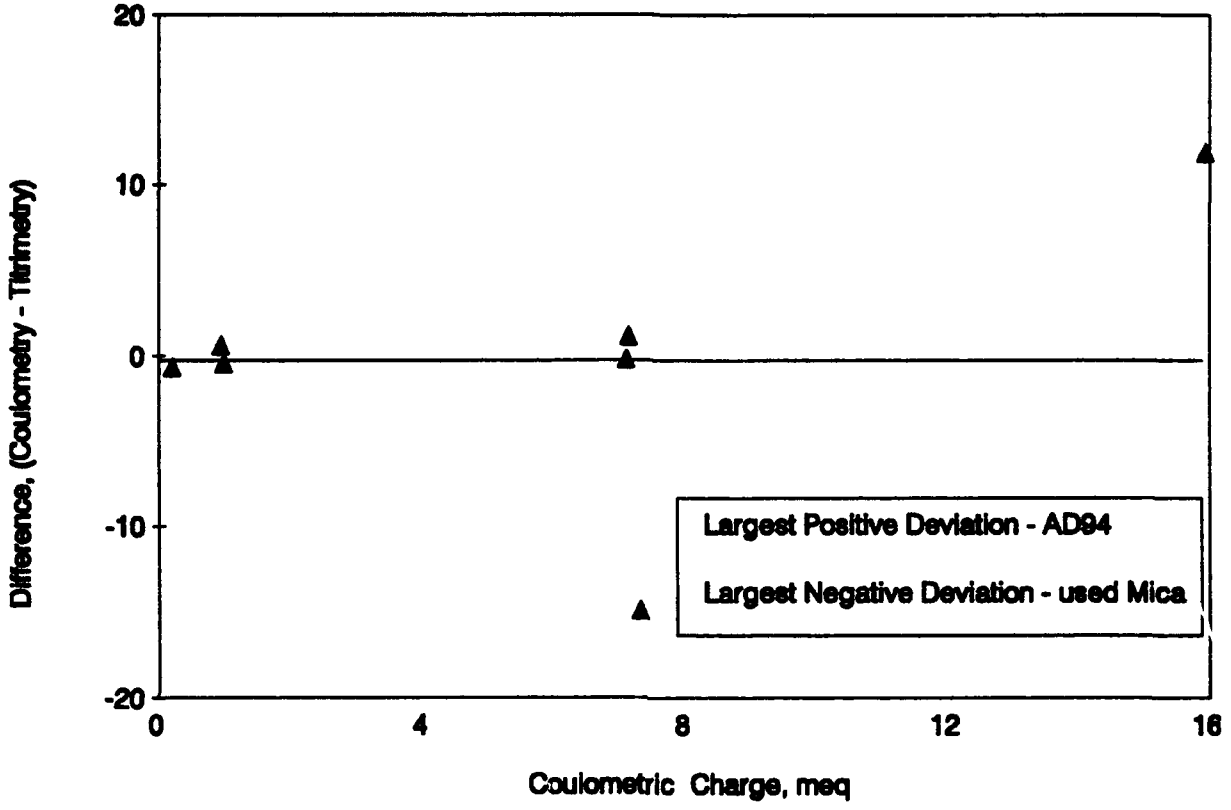

Figure 24. Comparison of Charge and Titre

The materials that are useful for battery applications that would not compromise lifetime are those with less than 2 meq of Li by UPD which are as follows:

- Cast LiF
- AlN
- BN

The data for all tests are given in Table 5. ARDEC module ML 08 had both LiF strips and BN felt as part of the bipolar edge seal mechanism. This module operated for 35 days, was subjected to 14 freeze-thaw cycles and delivered 324 cycles with 2186 pulses. Samples were taken from an interior cell and analyzed for Li by titrimetry. The Li content of the BN was 3.6% and that of LiF was 0.6% indicating Li transport in the cell, and, furthermore, that Li is not completely captured by LiF. In spite of this the module was long-lived and performed well. Coupling the testing and evaluation of the materials with the module performance serves as a calibration point for our data.

It is noted that in the case of " not previously used mica", that the gas formed when the insulator was placed in water was captured and measured. There was ignition suggesting elemental Li in the insulator, and this ignition caused a low reading error for the gas. The gas actually measured corresponded to 5.5 meq versus an expected 7.1 meq based on coulometry. It is deduced that about 1/4 of the hydrogen produced burned to water.

Boron nitride was another uniquely behaved material. In contact with water it hydrolyzed to H_3BO_3 and NH_4OH so that titration measures both the Li that caused a swelling of BN and the NH_4OH from the hydrolysis.

Table 5. Summary of Insulator Effect on Lithium Transport

ID	Insulating material	Coulometry, meq	Insulator titre, meq	"UPD" Mo, meq	Control Mo, meq	Gas Collection, meq	Lowest Current, uA	Deviation, Coul. - titre
LBCM 2075 *	Boron nitride	0.98	1.23	0.07	0.08		180	-0.4
LBCM 2076 **	Mica, used	7.31	22.1	0.03	0.09		1,250	-14.91
LBCM 2081	Mica	7.1	7.05	0.05	0.15	5.45``*	2,750	-0.15
9 83-9#10	Lithium fluoride	0.21	0.71```	0.09	0.05		135	-0.64
91083-9#8	Aluminum nitride	0.94	0.2	0.08***	0.04		220	0.62
91083-9#11	Alumina AD94	15.93	2.88	0.07	0.1		6,200	12.88
91083-9#12	Alumina AD995	7.13	0	5.9	0.03		450	1.2
ML 08	BN from module	3.60%						
ML 08	LiF from module	0.60%						

*Subsequent testing of BN rings indicates hydrolysis of BN to H_3BO_3 and NH_4OH.

**Mica corner from ARDEC 5 cell battery (via G. Barlow). Fizz from dark region. 0.28 g sample has 0.11 meq Li in part A. Part B 0.764 g sample 0.03 meq (see p. 38 book 170026 for parts A and B).

***A black particle was flipped off the molypop. If this was a Li nodule its weight was 4.7 mg and its size would be about 8 microliters.

```A control sample of LiF had zero titre (did not cause phenolphthalein to change color - the same result as with electrolyte).

``*Ignition was responsible for low results.

## VIII.Seal materials recommendations

Three materials are considered qualified as insulators in seal development which are:

- Cast LiF
- AlN
- Boron nitride.

BN should be freshly made and stored dry to avoid hydrolysis.

Underpotential deposition does occur and can cause (1) swelling and discoloration of insulators and (2) give rise to Li nodules on metals at the potential of the anode. A second necessary condition for UPD to occur is that the site be electrolyte covered hence, the corollary is that metal sites be dry or not at the
```

anode potential to avoid UPD. It is speculated that sufficient nodule growth or filling of the insulators the metal can ultimately become a failure mode. The current is a measure of nodule growth or of the diffusion rate of elemental Li from the deposition site into with the insulator.

IX.Conclusions

- CoS_2 has been shown to be the best cathode active material for high temperature pulse power cells. Although there are three distinct electrochemical reactions at the very high current densities involved, the two most energetic levels behave as a mixed potential discharge reaction. Because of this, we have succeeded, with thin electrodes, to achieve discharges corresponding to 1.4 Faradays per mole of CoS_2. In turn, this greater depth of discharge (previous baseline value was 1.08 Faradays per mole) enables the cells to be fabricated smaller and lighter resulting in stable pulse discharge operation at higher power densities.
- The mass of anode material could equivalently be decreased providing the theoretical capacity is based only on the β to α transition. Quantitatively the capacity has been increased from 145 mAh/g of active materials up to 180 mAh/g.
- The combined affect of the two previous conclusions above would result in an estimated reduction of the baseline 100 MJ system volume from 0.40 to ~0.36 m^3.
- Among the separators that may be substituted for Maglite D are silicon nitride, Magox Super Premium MgO, yttria and sintered AlN. The last material is dimensionally stable thereby easing battery module requirements and design. Additional work is required to successfully mate large area, 150 cm^2 AlN separators with slurry cast anodes and cathodes.
- To fully qualify these separator materials, multi-cell bipolar stack tests are needed to confirm cell balance and longevity.
- The newer separator materials show lower final currents, withstand freeze-thaw incidents yet enhance cycle life. Final currents, after somewhat extended charges, reach acceptable values ranging 5 mA/cm^2 to as low as 0.5 mA/cm^2.
- Li(alloy)/CoS_2 cells are capable of fast charging by increasing the initial charge rate. In fact, the electrochemical system behaves best when the initial charge rate is ~50 mA/cm^2 or greater.
- Self -discharge rates are much lower than in other molten salt systems, since an eight hour open circuit stand permits the first 10 of a series of 12 pulses to have minimal effects upon power. Reasons for this behavior include: greater thermal stability of CoS_2 (to 760°C) and no apparent solubility and mobility of the CoS_2 in the electrolyte (known to be a factor in the high self discharge experienced with primary thermal batteries employing FeS_2).
- Cell balancing can be upset by common electrolyte paths. These come about by battery compression and electrolyte migration. The mobility of the electrolyte can be controlled to a small extent by electrolyte management. The amount of electrolyte can be decreased by using dimensionally stable separators and by decreasing the electrolyte content in the anode from 35 w/o down to 27 w/o. If the electrolyte content is decreased below this value for the anode, or decreased below 20 w/o in the cathode, complete cell formation does not occur at pulse discharge rates.

- Since there remains an excess of electrolyte, a seal is needed to prevent formation of a common electrolyte pathway in the battery. The materials used as seals employ an insulator, and we discovered that Li can be transported via an underpotential mechanism and intercalate within the insulator. This discovery became a basis for a seal material screening process. A result of the screening process is that boron nitride, aluminum nitride and lithium fluoride are suitable materials for inclusion in the seal design.
- When placed on open circuit, the polarization decays and cell voltage recovers. If the system is deprived of the rest period by rapid sequential high rate pulsing, the voltage, hence power, of the system is affected by a 5% decrease in values.
- The accomplishments of the program are that the Li/CoS_2 system has been made (1) lighter in weight, (2) smaller in size, (3) to have an increased cycle life exceeding original goals, (4) to remain balanced for longer periods and (5) to be more reliable and reproducible.

These conclusions and their significance are summarized in Table 6 below.

Table 6. Summary and Significance of LABCOM Program Accomplishments

ACCOMPLISHMENT	*SIGNIFICANCE*
• Stable Pulse Discharge Performance Demonstrated Over 370 Cycles and One Calendar Month at Operating Temperature of 480 °C - Cell terminated after recharge conditions intentionally altered, resulting in cell failure - Demonstrated increased utilization of active materials over extended time period	• New Cycle Life Record Demonstrates No Inherent Cycle Life Limitations, Even With Increased Utilization of the Active Materials - Used Alternate and Readily Available MgO (separator) Source - MAGOX - SP - Potential to reduce overall system volume by ~10 to 15% or use thicker separators
• Established Critical Lower Bound on Recharge Current Density	• Verified That Recharge Current Densities of <50 mA/cm² Can Result in Rapid Cell Failure - Requires full size modules have sufficient heat removal capability on recharge to accept this current density without overheating - Modules tested to date used 50 mA/cm²
• Reproducibly Demonstrated No Loss of Voltage or Capacity After 8-hrs of Open Circuit Stand	• Feature Unique to CoS_2 Permits Active Stand-by Without Loss of Performance • Opens Up New Military Applications Such as Advanced, Active Sonobuoys
• Porous, *Dimensionally Stable* Aluminum Nitride (AlN) Separators Have Been Successfully Fabricated and Tested in a 20 cm² Cell • Initial performance outstanding • 100 cycles demonstrated with stable and reproducible performance • Lowest final currents observed (at 0.5-1.5 mA/cm²) will promote stack balance in multi-cell bipolar stacks	• Potentially Eliminates Two Casting and Three Pressing Steps in the Electrode Fabrication. Process • Highly Uniform Structure Free of Visible Imperfections Such As Pinholes Should Maximize Both Cycle and Calendar Life • Structural Stability Will Reduce Axial Dimensional Changes During Cycling • High Thermal Conductivity Will Promote Heat Transfer and Simplify Thermal Management in Full Size Modules

• Decreased Final Currents	• Battery cells remain in balance

Table 6. Summary and Significance of LABCOM Program Accomplishments (continued)

ACCOMPLISHMENT	*SIGNIFICANCE*
• Common Electrolyte Model	• Verified importance of edge seal and electrolyte management - contributes to cell balance - contributes to longevity
• Underpotential Deposition	• Identified a failure mode - established a test for edge seal material evaluation - relationship to electrolyte management demonstrated

X. References & Endorsements

B.A. Boukamp, et. al., J. Electrochem. Soc., 128, 725 (1981)
R.A. Huggins, ANL-86-40, Proc. Int. Workshop on High Temp. Molten Salt Batteries.
D.E. Harney, U.S. Patent 4,221,849, Sept. 9, 1980
ANL 77-75, ANL 8039, ANL Quarterly Report to EPA, April 1971.
D.R. Vissers, et. al., Lithco Symp. on Lithium Chem., Ed. R. Bach, John Wiley and Sons, N.Y.
M. Williams, et. al., Proc. 32nd Power Sources Conf., p 658 ff (1986).
C.D. Desjardins and G.K. MacLean, Abstr. 52, Electrochem. Soc. Mtg., Oct. 1989.
T. Kaun, et.al., Abstr. 47, Electrochem. Soc. Mtg. ,Oct. 1988.
T. Leegaard and T. Rosenqvist, Z. Anorg. Chemie, 138, 294 (1964).
E.S. Takeuchi and W. C. Thiebolt, J. Electrochem. Soc., 138, L144 (1991).
$Mo = Mo^{+3} + 3e^{-}$ -0.2 volts
H. Maraqah et. al., J. Electrochem. Soc., 138, L61 (1991)
Uniformity is macroscopic and not microscopic as determined by study of radiocolloids.
Interchange of ions and its elements can occur and has been established using radioisotopes.

Electronics Technology and Devices Laboratory
Mandatory Distribution List
Contract or In-House Technical Reports

Defense Technical Information Center *
ATTN: DTIC-FDAC
Cameron Station (Bldg. 5)
Alexandria, VA 22304-6145

*(Note to Contractor: Two copies for DTIC will be sent from the STINFO Office, Fort Monmouth.)

Director
US Army Material Systems Analysis Actv
ATTN: DRXSY-MP
001 Aberdeen Proving Ground, MD 21005

Commander, AMC
ATTN: AMCDE-SC
5001 Eisenhower Ave.
001 Alexandria, VA 22333-0001

Commander, LABCOM
ATTN: AMSLC-CG, CD, CS (in turn)
2800 Powder Mill Road
001 Adelphi, MD 20783-1145

Commander, LABCOM
ATTN: AMSLC-CT
2800 Powder Mill Road
001 Adelphi, MD 20783-1145

Commander,
US Army Laboratory Command
Fort Monmouth, NJ 07703-5601
1 - SLCET-DD
1 - SLCET-DT (M.Howard)
1 - SLCET-DR-B
22 - Originating Office

Commander, CECOM
R&D Technical Library
Fort Monmouth, NJ 07703-5703
1 - ASQNC-ELC-IS-L-R (Tech Library)
3 - ASQNC-ELC-IS-L-R (STINFO)

Advisory Group on Electron Devices
ATTN: Documents
2011 Crystal Drive, Suite 307
002 Arlington, VA 22202

Electronics Technology and Devices Laboratory
Supplemental Contract Distribution List
(Elective)

Director
Naval Research Laboratory
ATTN: Code 2627
001 Washington, DC 20375-5000

Cdr, PM JTFUSION
1500 Planning Research Drive
001 McLean, VA 22102

Rome Air Development Center
ATTN: Documents Library (TILD)
001 Griffis AFB, NY 13441

Deputy for Science & Technology
Office, Asst. Sec. Army (R&D)
001 Washington, DC 20310

HQDA (DAMA-ARZ-D/
Dr. F.D. Verderame)
001 Washington, DC 20310

Dir, Electronic Warfare/Reconnais.
Surveillance & Target Acquis. Dir.
ATTN: AMSEL-RD-EW-D
001 Fort Monmouth, NJ 07703-5206

Dir, Reconnais. Surveillance &
Target Acquisition Systems Dir.
ATTN: AMSEL-RD-EW-DR
001 Fort Monmouth, NJ 07703-5206

Cdr, Marine Corps Liaison Ofc.
ATTN: AMSEL-LN-MC
001 Fort Monmouth, NJ 07703-5033

Dir, US Army Signals Warfare Dir.
ATTN: AMSEL-RD-SW-OS
Vint Hill Farms Station
001 Warrenton, VA 22186-5100

Dir, CECOM Night Vision &
Electro-Optics Directorate
ATTN: AMSEL-RD-NV-D
001 Fort Belvoir, VA 22060-5677

Cdr, Atmospheric Sciences Lab
LABCOM
ATTN: SLCAS-SY-S
001 White Sands Missile Range, NM
88002

Cdr, Harry Diamond Laboratories
ATTN: SLCHD-CO, TD (in turn)
2800 Powder Mill Road
001 Adelphi, MD 20783-1145

Naval Surface Weapons Center
Code R-23
ATTN: Patricia Smith
001 Silver Spring, MD 20902-5000

US Army Armament Research,
Development & Engineering Ctr.
Picatinny Arsenal, NJ 07806-5000
1 - SMCAR-FSE (Dr. A. Graf)
1 - SMCAR-FSE (Ms. Laura
Krzastek)
1 - SMCAR-FSC (Ms. H. Naber-
Libby)